

DOCKETED

Docket Number:	21-BSTD-01
Project Title:	2022 Energy Code Update Rulemaking
TN #:	237688
Document Title:	Tracer Gas Capture Efficiency Test Method
Description:	Authors: I.S. Walker, J.C. Stratton, W.W. Delp, and M.H. Sherman. Lawrence Berkeley Nation Laboratory. February 2016.
Filer:	Adrian Ownby
Organization:	California Energy Commission
Submitter Role:	Commission Staff
Submission Date:	5/6/2021 9:00:22 AM
Docketed Date:	5/6/2021



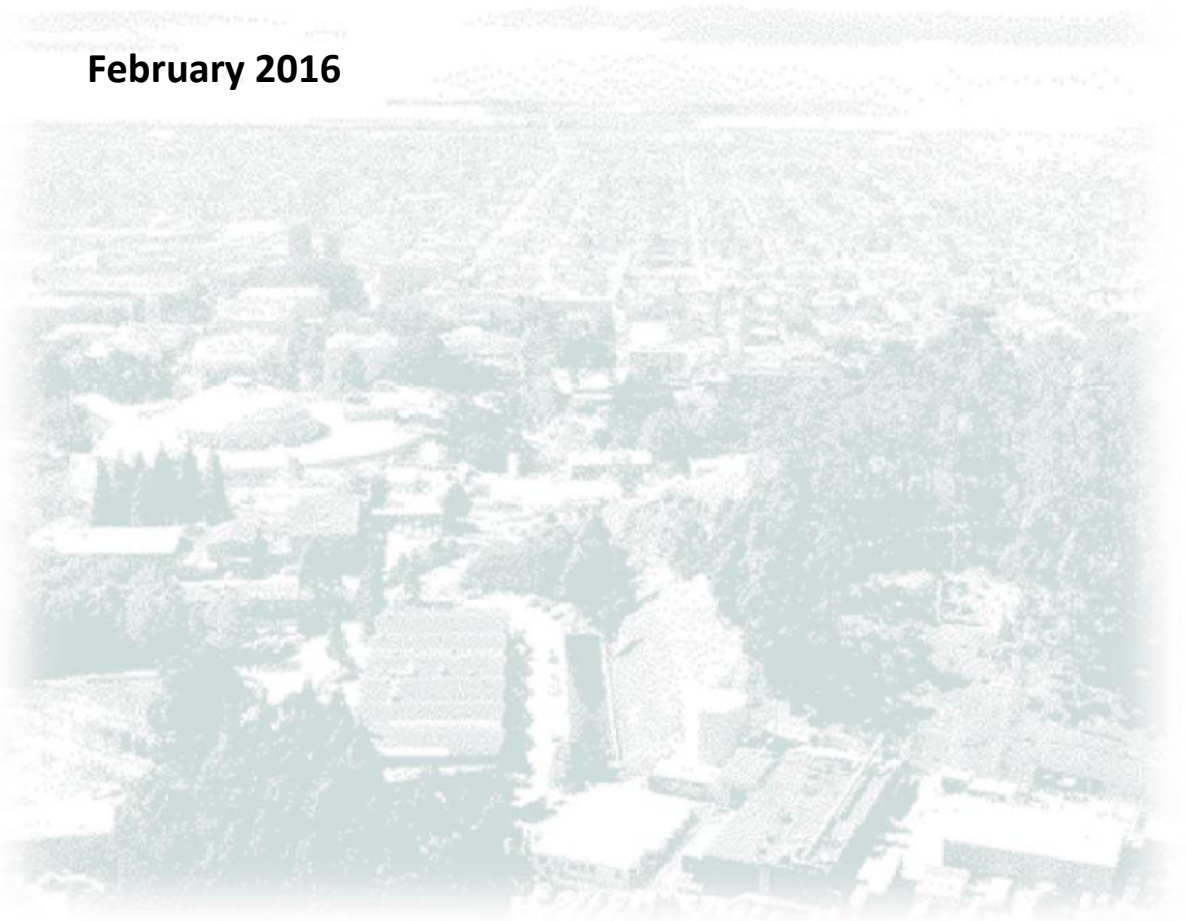
ERNEST ORLANDO LAWRENCE BERKELEY NATIONAL LABORATORY

Development of a Tracer Gas Capture Efficiency Test Method for Residential Kitchen Ventilation

I.S. Walker, J.C. Stratton, W.W. Delp, M.H. Sherman

Environmental Technologies Area

February 2016



Disclaimer

This document was prepared as an account of work sponsored by the United States Government. While this document is believed to contain correct information, neither the United States Government nor any agency thereof, nor The Regents of the University of California, nor any of their employees, makes any warranty, express or implied, or assumes any legal responsibility for the accuracy, completeness, or usefulness of any information, apparatus, product, or process disclosed, or represents that its use would not infringe privately owned rights. Reference herein to any specific commercial product, process, or service by its trade name, trademark, manufacturer, or otherwise, does not necessarily constitute or imply its endorsement, recommendation, or favoring by the United States Government or any agency thereof, or The Regents of the University of California. The views and opinions of authors expressed herein do not necessarily state or reflect those of the United States Government or any agency thereof, or The Regents of the University of California.

Funding was provided by the U.S. Dept. of Energy Building Technologies Program, Office of Energy Efficiency and Renewable Energy under DOE Contract No. DE-AC02-05CH11231; by the U.S. Dept. of Housing and Urban Development Office of Healthy Homes and Lead Hazard Control through Interagency Agreement I-PHI-01070, and by the California Energy Commission through Contract 500-08-061.

Ernest Orlando Lawrence Berkeley National Laboratory is an equal opportunity employer.

Acknowledgements

The authors would like to acknowledge the contributions of Brett Singer, Spencer Dutton and Rick Diamond to this report.

I. Introduction

Cooking activities produce a high quantity of water-vapor, which increases the indoor air moisture level and substantially contributes to indoor air quality problems (from the increase of water-condensation and mold) causing health problems for the occupants, such as asthma and allergies. Cooking also produces fine and ultrafine particles and a wide range of irritant and potentially harmful gases including acrolein and polycyclic aromatic hydrocarbons. Combustion products from fuels add to these pollutant sources. The purpose of kitchen ventilation is to remove pollutants, moisture, smoke and odors generated during cooking. A good overview of the need for kitchen ventilation is provided by Parrott et al. (2003). Air pollutants emitted during food preparation and burner operation include the following: carbon monoxide (CO), nitrogen dioxide (NO₂), formaldehyde (CH₂O) and ultrafine particles (UFP) produced by gas burners (Rim, Wallace, Nabinger, & Persily, 2012; Singer et al., 2010); UFP from electric heating elements (Dennekamp et al., 2001); and volatile organic compounds (VOCs) and particulate matter – including UFP and fine particulate matter mass (PM_{2.5}) – released during food preparation (Booth & Betts, 2004; See & Balasubramanian, 2008). Water vapor is generated by gas burners and released during many cooking activities.

Kitchen ventilation can be provided via any of the following system designs: range hood or other exhaust device – including a combination microwave range hood – mounted above the cooktop; downdraft exhaust system mounted alongside the cooktop burners; exhaust fan in the room containing the kitchen; exhaust fan elsewhere in the home. Since the goal of kitchen ventilation is to remove moisture and pollutants from the location within the house where they are being released, kitchen ventilation is most effective when it is closest to moisture and pollutant sources. A range hood, downdraft exhaust vent and potentially even a well-placed wall or ceiling exhaust fan can be much more effective than an exhaust fan placed elsewhere in the kitchen or home.

The most common way of providing kitchen ventilation is via a range hood mounted over the cooktop. Many building codes require installation of range hoods in new construction. Indoor air quality standards specify the required air flow rates for range hoods, as that is the only performance metric commonly available. For example, ASHRAE 62.2 (2013) specifies a minimum of 100 cfm (50 L/s) together with a sound rating of 3 sone, or less. The Home Ventilation Institute provides a directory of products that can be used to select kitchen range hoods that meet these requirements (HVI, 2015).

Current standards use air flow as a metric of interest when considering kitchen ventilation, however, air flow alone does not tell us how much of the cooking pollutants are exhausted to outside by the range hood. A better metric is capture efficiency. Capture efficiency is the fraction of pollutants emitted by the cooking that are vented directly to outside. A capture efficiency of 100% means that zero cooking pollutants enter the home. Note that there are secondary effects for any capture efficiency below 100%: any pollutants that do enter the home will still be diluted by the air flow into the kitchen induced by the range hood. This secondary effect is not included in our definition of capture efficiency. This keeps the definition and our ability to measure capture efficiency simple and direct – i.e., not dependent on other air flows or ventilation systems that may (or may not) be operating in the home.

Existing test methods for commercial kitchen hoods (ASTM, 2005) use flow visualization techniques (Schlieren photography) to check that the whole plume of pollutants from the cooktop is captured by the hood. However, they are very difficult to adapt to the estimation of partial capture characteristic of residential range hoods. For residential range hoods we are not going to require 100% capture because there is much less cooking in residential applications and the air flow required (and corresponding tempered make-up air), hood space requirements and hood placement are too difficult and expensive to achieve in homes. Therefore we did not use these existing commercial range hood testing procedures.

There is a European standard for range hood performance (IEC, 2005) that includes fan performance, grease absorption and odor extraction. Another European standard includes a range hood rating metric that looks at reductions in room concentrations of a volatile tracer due to ten minutes of range hood operation compared to the concentration with the range hood not operating. Some aspects of this standard are used in the test method developed in this report: the use of a tracer gas emitted into a heated plume, the mounting of the range hood inside a test chamber, and specifications for cabinetry to mimic a kitchen. Like the commercial test methods, this European standard does not give us the metric we are interested in: the fraction of cooking pollutants directly exhausted by the range hood.

The performance of residential range hoods has been examined in some previous studies. Kuehn et al. (1989) performed laboratory experiments that used flow visualization. Their results showed how air flow rate and geometry effects changed the air flow patterns into the hood and room, e.g., downdraft hoods were significantly less effective and the addition of side baffles improved performance. In addition, they investigated the airflow patterns for range hoods using both analytic models and laboratory measurements. Work by Fugler (1989) focused on air flow performance and found that average airflows for hoods installed in kitchens were only 35% of their rated flow. Rim et al. (2012) looked at reductions in particle concentrations from gas cooking in homes and found that range hood operation reduced particle concentrations by 31-98% depending mostly on the air flow through the hood. Li and Ho (2001) investigated the use of a two-zone approach to modeling range hood capture in a room (based on previous work by Li and Delsante (1996) that was attempting to model the contaminants captured directly and that entrained from the room), in which the space is divided into a room zone and a cooking region near the cooktop. They also performed laboratory experiments that showed that at low air flows (about 20 L/s) capture efficiency decreased with increased heat power input and that the modeling significantly overpredicted capture efficiency.

Previous studies by LBNL (Singer, Delp and Apte, 2010 & Singer, Delp, Price and Apte, 2012 & Delp and Singer, 2012) have shown that the physical shape and design of range hoods can change their capture efficiency. To evaluate the test method over a reasonable range of these parameters, eight wall-mounted range hood models were tested using the new test procedure. This first round of testing is focused on wall-mounted range hoods because they are the most common (Klug, Singer, Bedrosian, & D'Cruz, 2011). In the future we plan to adapt the method for use with downdraft exhausts and island hoods.

This test method has been created with the intent of it being used in an ASTM test method such that range hoods can be evaluated. The development has included input from the ASTM working group responsible for writing the ASTM test method. This group includes manufacturers of range hoods, researchers, and potential users of the standard.

II. Test Method

The range hood to be tested is mounted on a wall above a combined heat source and tracer gas emitter. The heat source has dimensions and power output intended to mimic a cooking event. The tracer gas is used to seed the thermal plume above the heat source. The test is performed inside a test chamber such that, after a few minutes of operation, the tracer gas concentrations have reached equilibrium. This allows for a simplified mass balance calculation that reduces the errors arising from uncertainties in the tracer gas analyzer. The test chamber dimensions were chosen to be similar to those used in existing standards for residential range hood testing. This will make it easier for more people to perform the testing in the future. The dimensions approximate a small kitchen.

There are many parameters that vary during a cooking event and the test method aims to address the key ones: the number of burners operating, the heat output of each burner, the geometry of the plume from each burner and how it interacts with the pot. The following discussion focuses on creating a test method that is consistent while retaining features that are typical/common in cooking without being too extreme. It is possible to test under extreme cases of all burners on full, or only one burner on very low, but the principle followed here was to select conditions that were not extreme and might represent many typical cooking events. This way we have a capture efficiency that is focused on the commonest events, which is preferable if the test is to be used for standards or codes interested in public health.

Some preliminary experiments were performed using natural gas burners as the source of heat on the cooktop. However, there were several concerns that led to the use of electric elements: higher fire hazard than electricity plus additional safety concerns regarding supply and or storage of gas fuel, the range of shapes and design of available gas burners would reduce consistency between different test set-ups (it was deemed to be too difficult/restrictive to specify a particular burner and gas flow rate), and the ease of monitoring and recording power output of electric elements. Based on manufacturer surveys and discussions with the ASTM working group two electric heating elements are operated simultaneously – one at the back of the cooktop and one near the front. The elements are set to a medium level (roughly 1900W total power output) that keeps the temperature at the tracer gas injection point at about 200°C. Some previous experiments at LBNL (Singer et al. 2011) and by other researchers used pots of boiling water on the elements or gas burners. These boiling water pots are not used in the test method for several reasons:

- Boiling water leads to experimental and potential safety issues with water condensation in the ducts, test chamber and instrumentation during testing. In addition, one of the most likely tracer gasses to be used in the experiment is CO₂ for safety and cost reasons, and CO₂ sensors are often sensitive to water vapor and would make the tracer gas measurements have greater uncertainty.
- Much of the heat goes into phase change for the water rather than the hot plume above the cooking surface. Eliminating the boiling water allows the use of lower power, which is good from a safety perspective, while maintaining the same heat input to the plume.
- The use of pots means that pot dimensions need to be strictly defined for consistency between tests and this can lead to difficulties in adoption unless standardized pots are made available.

Even though there is no boiling water, and therefore no pot, there is the need to create a plume geometry that is close to a typical cooking event. A naked element is physically smaller in diameter than most cooking pots, so an iron plate larger in diameter than the element was used to mimic the spread of

the hot plume radially around the bottom of a pot. Lastly, there was the need to inject tracer gas across the whole cross section of the thermal plume and not just inside the pot. If the tracer gas is only injected inside the pot, then the core of the plume receives more tracer than the periphery and this would tend to bias the capture efficiency high. Conversely, when gas burners were used and the tracer gas was the CO₂ from combustion, this tended to seed only an annulus around the perimeter of the plume and this could potentially bias the capture efficiency to be too low. Therefore, the test method requires that the tracer gas be injected over an area of specific diameter to avoid these complications and sources of error.

Another parameter that influences CE is the height of the range hood above the cooktop. Manufacturers' recommendations cover a wide range of highest and lowest mounting heights. In the testing of range hoods the manufacturer's maximum and minimum heights were used. It is likely that the ASTM test method will specify some minimum height above the cooktop because some range hoods (microwave range hoods) have allowed mounting heights that are so low that they would interfere with the placement of reasonably sized pots on the cooktop and also expose the bottom of the range hood to excessive heat. In our experiments we melted the bottom of one microwave range hood despite following manufacturers' instructions.

Previous experiments (Lunden et al. 2014, Delp and Singer 2012, Singer et al. 2012, Rim et al. 2012) have shown that capture is almost always better from rear burners than front burners. If it were possible to know which burners were used in cooking then we might be able to select either front or back burners for testing. However, different cooking events result in different pot placement. For example, slowly cooking for a long time (making soup, boiling beans) that requires little intervention from the cook would likely use a back burner, but stir frying that required constant attention from the cook is more likely to be done on a front burner. As a compromise, the test method uses one back and one front burner (on a diagonal: left front/right rear or right front/left rear) – with both burners operating simultaneously.

The capture efficiency calculation is based on measurements of tracer gas concentrations and performing a steady-state mass balance on the test chamber. It would be possible to do the analysis without waiting for steady-state, but this would require additional measurements of air flow rates and introduce additional uncertainty into the calculations. A key advantage of using ratios of differences in concentrations is that bias errors cancel out (assuming the same piece of equipment is used to measure the tracer gas concentrations at all locations). The capture efficiency of the device under test is calculated using the concentration of the tracer gas at three locations: inside the test chamber (C_c), at the test chamber inlet (C_i), and in the exhaust ducting (C_e). The formula to calculate capture efficiency (CE) is:

$$CE = \frac{C_e - C_c}{C_e - C_i}$$

Equation 1

Although this equation yields a fraction, for convenience in this report the Capture Efficiency is expressed as a percentage.

III. Apparatus

The test apparatus consists of a test chamber, an adjacent monitoring area, and exhaust ducting to outdoors. The exhaust ducting includes inline devices that enable both the measurement and control of airflow.

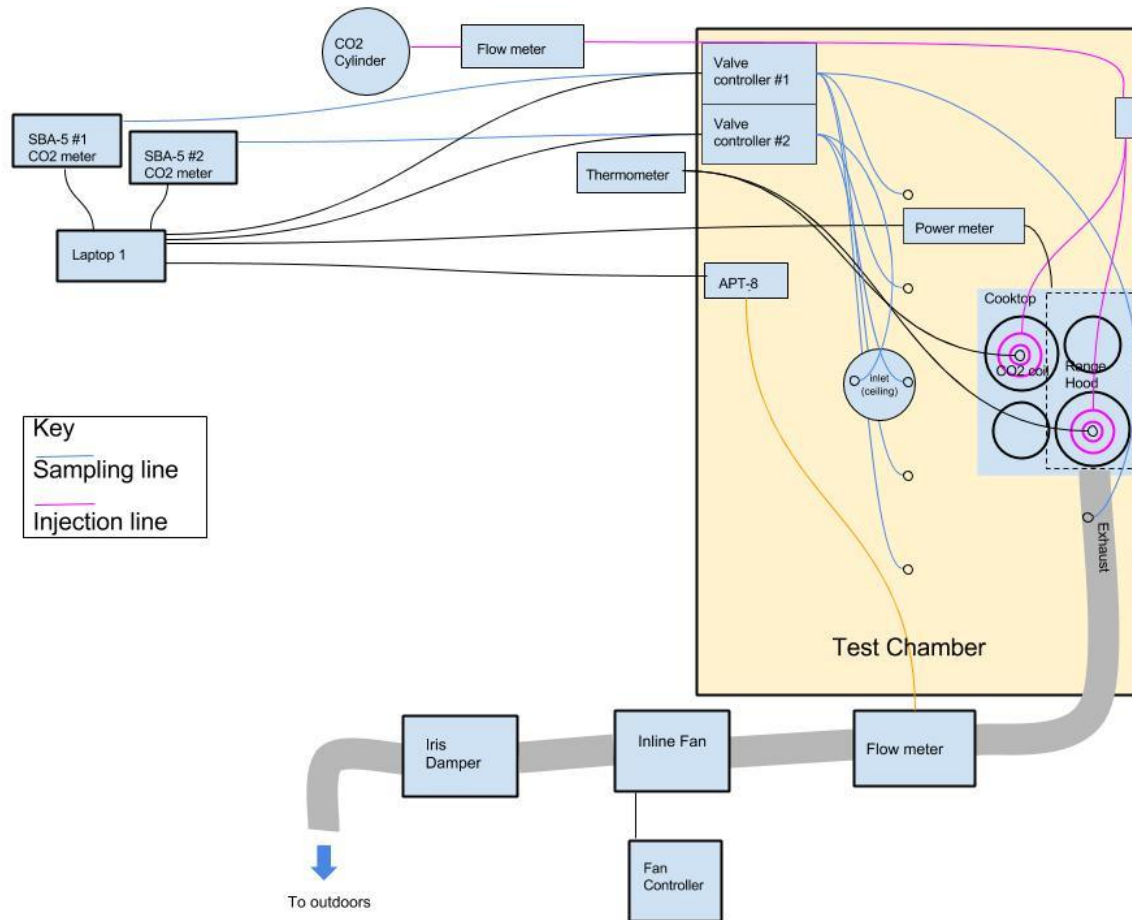


Figure 1: Schematic diagram of capture efficiency test apparatus

Figure 1 is a plan view of the test apparatus. The internal dimensions of the test chamber are: approximately 2 m x 3 m in floor plan and 2.4 m high. The chamber was air sealed so that almost all the air entering the chamber to make up for the range hood exhaust came through a known inlet whose concentration of tracer gas was measurable. This improves the accuracy of the concentration of tracer in the air entering the chamber. The air leakage was measured by sealing the inlets and outlets and pressurizing the chamber to 50 Pa. In volume normalized terms the air leakage was 2.5 ACH₅₀. Centered along one of the long walls of the test chamber is a four-burner electric range that is 76cm wide, 65 cm deep, and 90 cm tall. A 25.4 cm diameter inlet is centered in the chamber's ceiling. Suspended 4.5 cm below the inlet aperture is a 30.5 cm x 30.5 cm diffusion plate to prevent inlet air blowing directly in the hot air plumes and changing the air flow patterns due to range hood operation.

The range hood outlet passes through 22 cm diameter duct that exits the chamber out the ceiling and makes a 90-degree bend to run parallel to the chamber's flat roof. An inline fan and damper are used to control the air flow through the range hood. The duct exiting the chamber tapers to 15cm diameter then passes through a flow nozzle to measure the flow, then expands to 25 cm diameter and connects to the

inline fan. All ducting is rigid unless noted otherwise. Downstream of the inline fan is 25 cm diameter flexible ducting that leads to and terminates at a 25 cm diameter iris damper that is mounted in an exterior window. The supplemental inline fan and iris damper are shown in Figure 2. The kitchen cabinetry and the tested range hood were installed on the longest wall of the test chamber (see Figure 5). Two cabinets were located on the side of the range hood. The range hood was installed according to manufacturer's instructions at both lower and higher distance between the bottom of the range hood and the cooktop. A commercially available residential kitchen range was used for the experiments. The range used has two 0.14 m diameter heating elements with 1250 w power capacity and two 0.17 m diameter heating elements with 2100 w power capacity. The two 2100 w-capacity heating elements were used for the capture efficiency tests. On each side of the range are simulated countertops with cabinetry below. Simulated cabinetry is also mounted to the wall on either side of the range. Above the range, suspended from the ceiling is an adjustable-height range hood mounting assembly. Figure 3 and Figure 4 illustrate the location of inlets, outlets, cabinetry and the cooktop inside the test chamber. The figures also show the location of the tracer gas measurement locations: at the inlet, in the outlet of the range hood and in the room.



Figure 2. Inline fan and damper used to control air flows

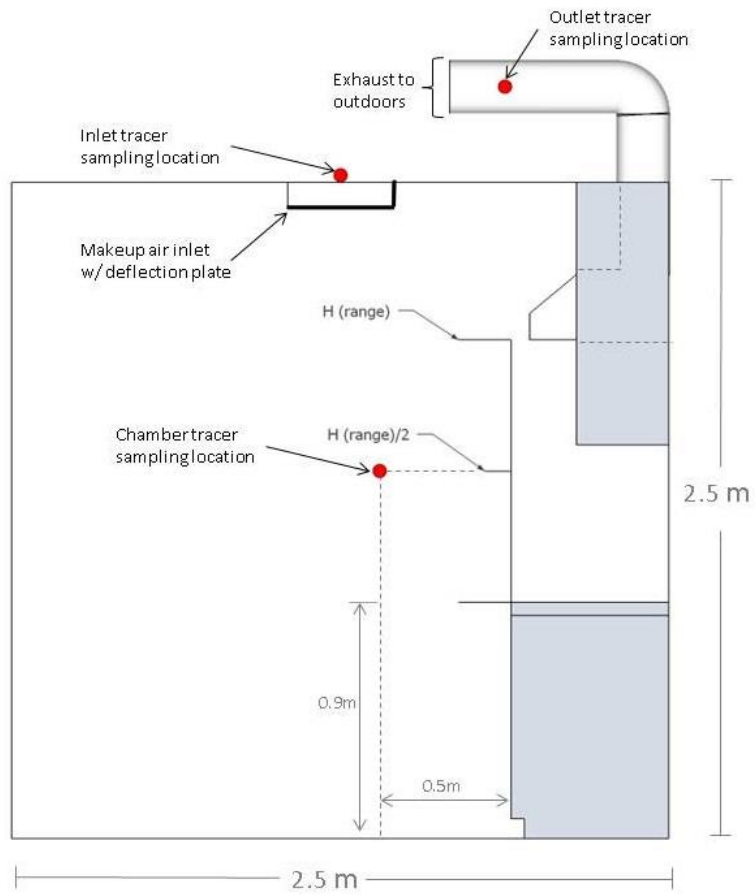


Figure 3. Sketch of test chamber – section

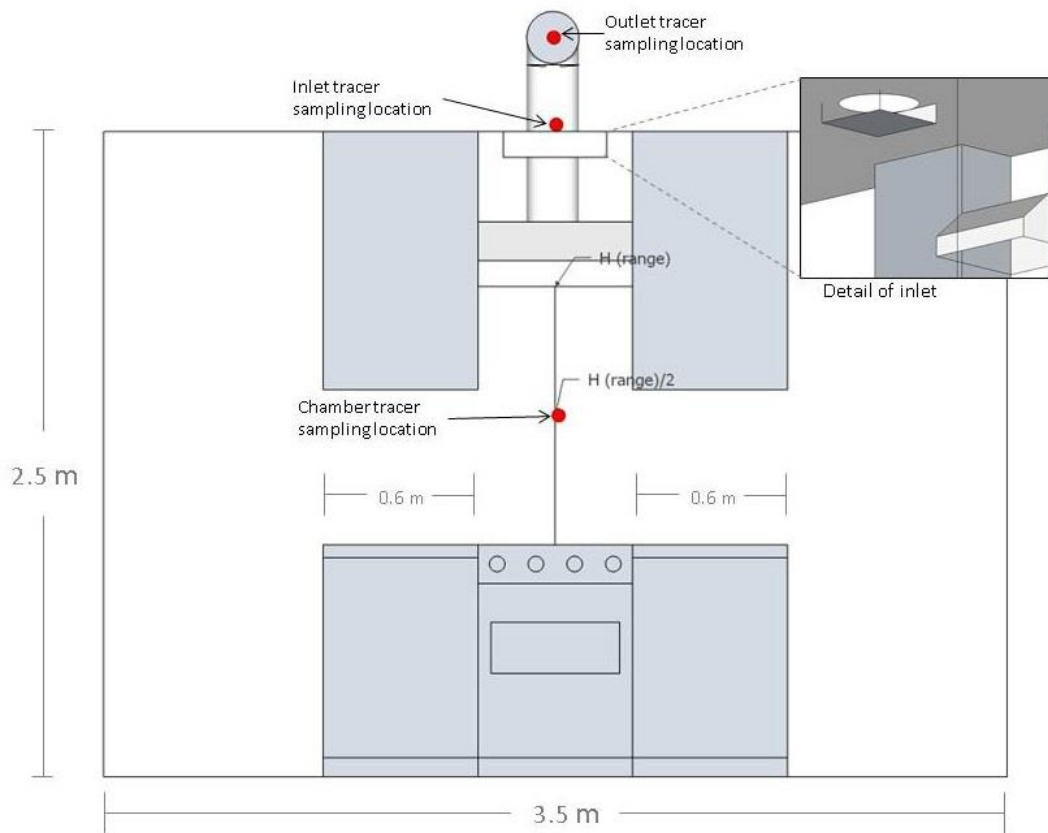


Figure 4. Sketch of test chamber - elevation

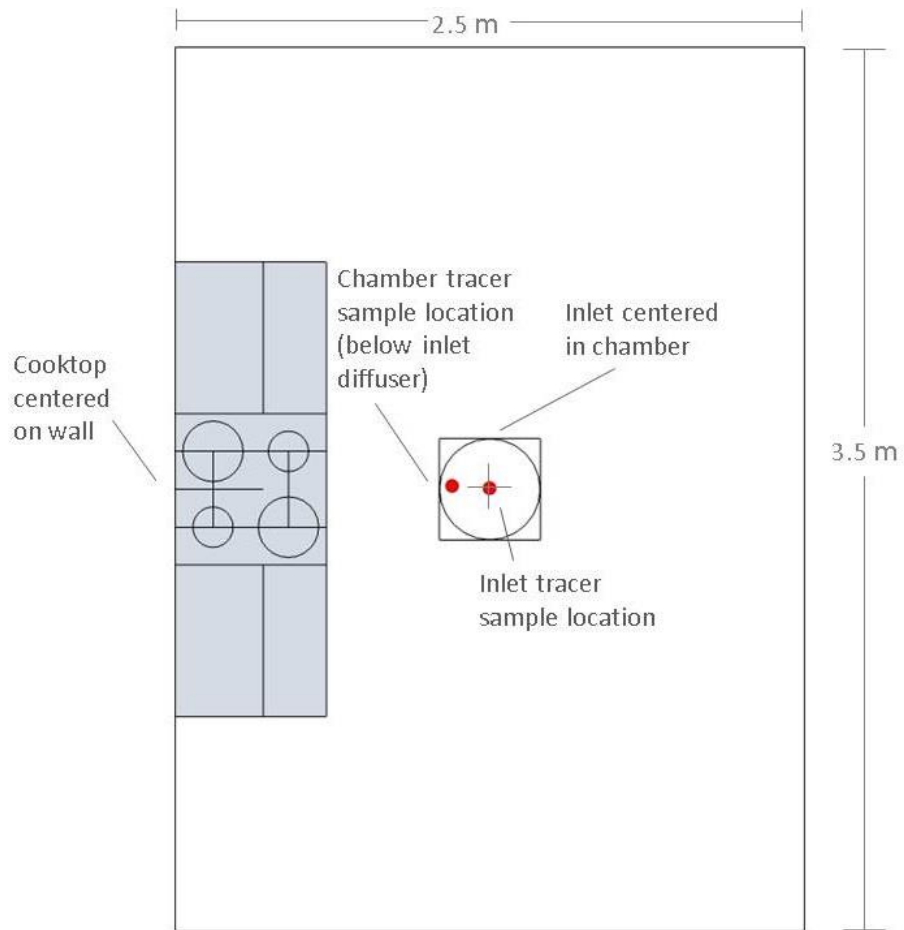


Figure 5. Sketch of test chamber - plan

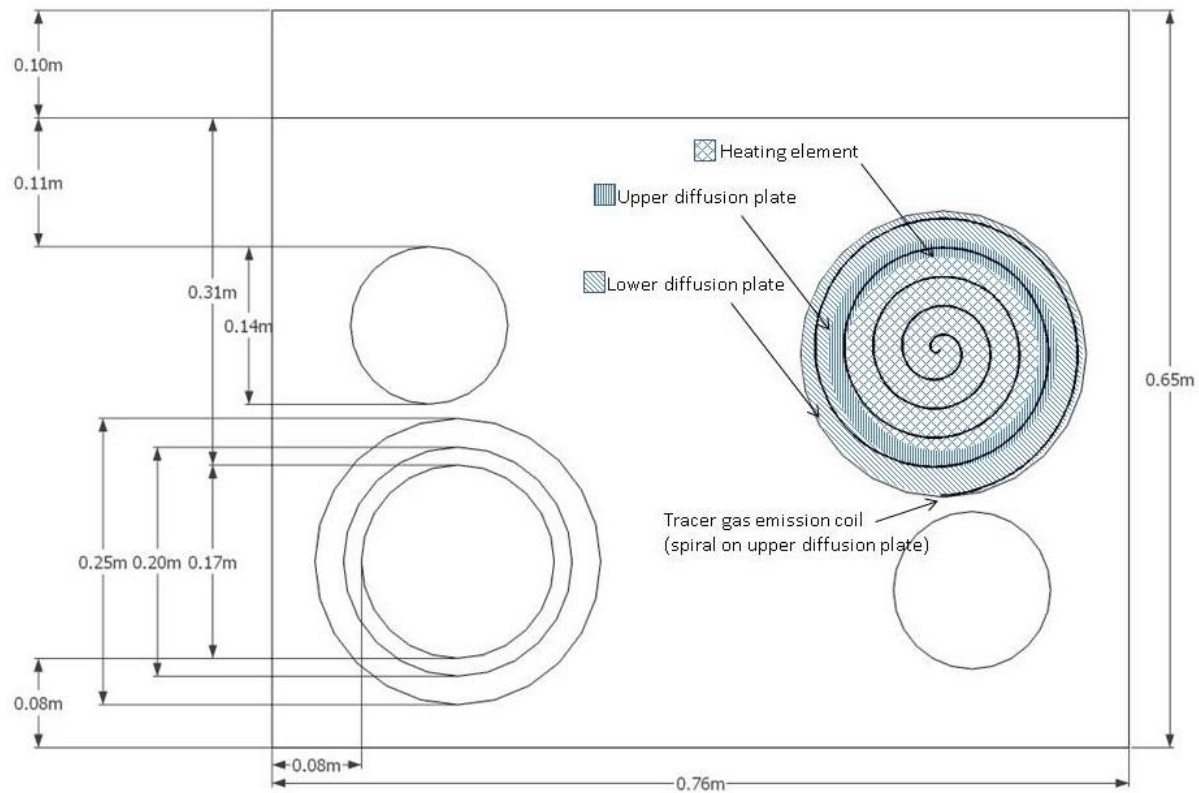


Figure 6: Plan view of cooktop and diffusion/emitter assembly

Preliminary Testing

Preliminary testing was done for several cooktop powers outputs, surface temperatures and pan locations (both single and two-pan configurations). Table 1 shows how the capture efficiency varies with these parameters. For more information and discussion of these preliminary tests see Simone et al. (2015). The results of the preliminary tests in Table 1 show that pans at higher temperatures have lower CE than pans at lower temperatures and pans on front burners have lower CE than pans on rear burners. This led us to choose a setup with two burners diagonally across from each other, one front and one back, and to choose a pan surface temperature that resembled those present when cooking: 200 °C. The power inputs for these preliminary tests were considerably lower than the later tests (even though the surface temperature is the same or higher) because there was no separation between the heating element and the pan.

Table 1: Preliminary Test results for a microwave exhaust hood at different thermal surface temperature and position of the pollutant pan-source.

Cooktop power (W)	Surface temperature (°C)	Source location	CE
213	200±5	Front	0.88
520	450±5	Front	0.52
212	200±5	Back	0.97
520	450±5	Back	0.94
405	200±5 (per spot)	Front & Back	0.76
1022	450±5 (per spot)	Front & Back	0.71

We want the measured tracer gas concentration in the room to be representative of the tracer gas concentration in the air entering the plume. Given the expected variation in tracer within the room we examined the special variability in the preliminary test setup by using twenty separate carbon dioxide measurement devices located throughout the test chamber and in the exhaust and inlet streams, as shown in Figure 6. The concentrations at the extremes near the chamber walls or near the floor did not have concentrations representative of those entering the plume. The concentrations under the cabinets showed large fluctuations as the uncaptured plume meandered intermittently through this part of the test chamber making these locations unsuitable for sampling. For these reasons, in subsequent testing, the sampling was focused near the range hood at a distance into the room that a person might stand at and that represents the air entering the plume from the room. For simplification and standardization of testing, a single reference measurement location is desirable. This will allow for easier replication in other test laboratories and make the test easier to standardize in a method of test. A reference location was selected that is on the horizontal centerline of the range hood, 0.5m into the room and vertically half way between the bottom of the range hood and the cooktop.

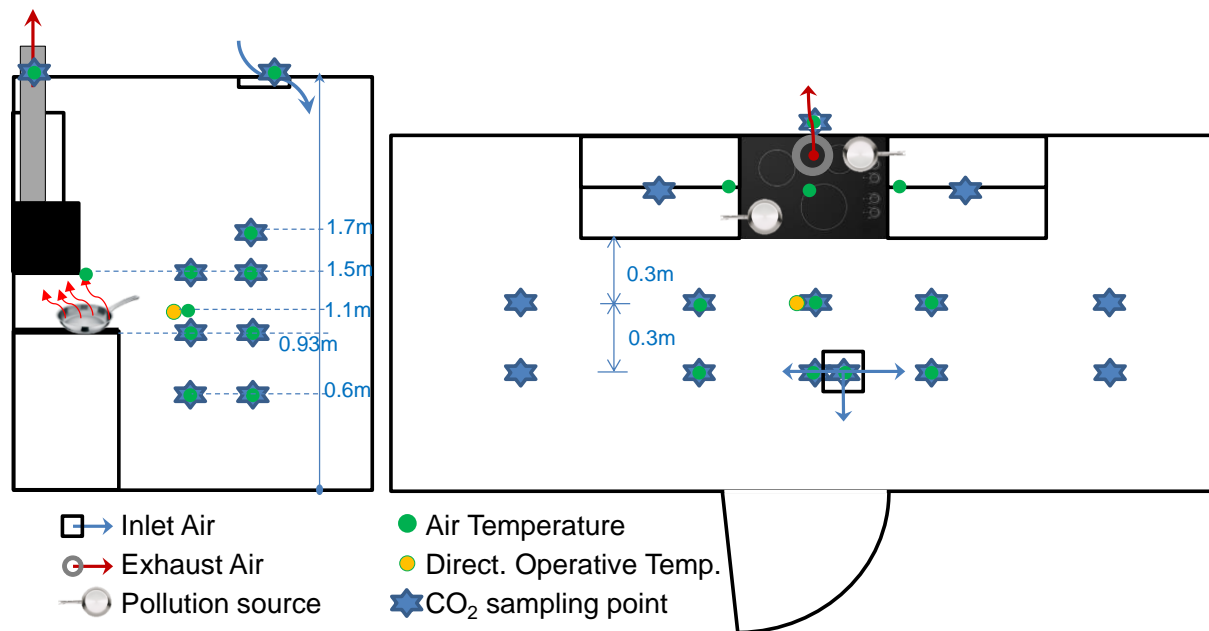


Figure 7: Section and plan of the test-kitchen reporting the measuring points and pollution source location for the preliminary testing.

This preliminary setup was effective in getting an initial survey of tracer variability in the test chamber, but had some downsides as a long-term setup for multiple tests. Because each location was measured using a separate analyzer, each analyzer had to be cross-calibrated against a higher accuracy device to correct for biases. A calibration factor was established for each individual device and applied to each of the individual measurements. Manually gathering data from each individual device for each test was time consuming and introduced the possibility of transposing data.

For these reasons, for the full scale testing we decided to change the sampling setup to use just two, high accuracy, auto-zeroing analyzers attached to a programmable multi-port valve controller. A Python script was written to monitor and record the port location and tracer gas concentration for each analyzer. This change increased the accuracy of our measurements and simplified and automated the data collection process.

Tracer Gas Injection

CO₂ was used as a tracer gas and injected through small holes in spirals of copper tubing. Figure 8 illustrates the arrangement of these injection spirals inside the pans. The spirals cover a circular area 18 cm diameter inside the 20 cm diameter pan. The tube used for the spiral had an external diameter of 0.5 cm and 21 pin holes of diameter 0.1 cm equally distributed over the area of the pan. This approach might not effectively seed the entire plume because heated air flowing around the outside of the pan and the perimeter of the pan are not seeded. Another issue with the use of commercially available pans is that it may be difficult to exactly replicate in other test facilities and is difficult to specify with enough precision in standards. Therefore, in future testing this system will be replaced by machined plates that can be accurately reproduced and an injector spiral that seeds the whole flow. Figure 9 illustrates an example of this approach and an overhead view is shown in Figure 8.

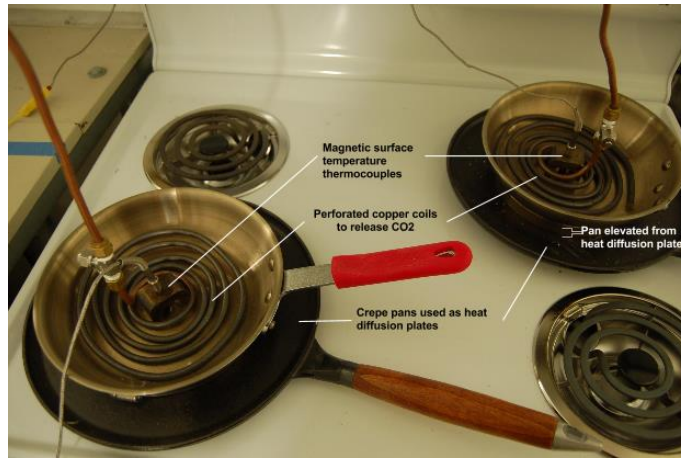


Figure 8: Tracer gas injection coils in pans on cooktop.

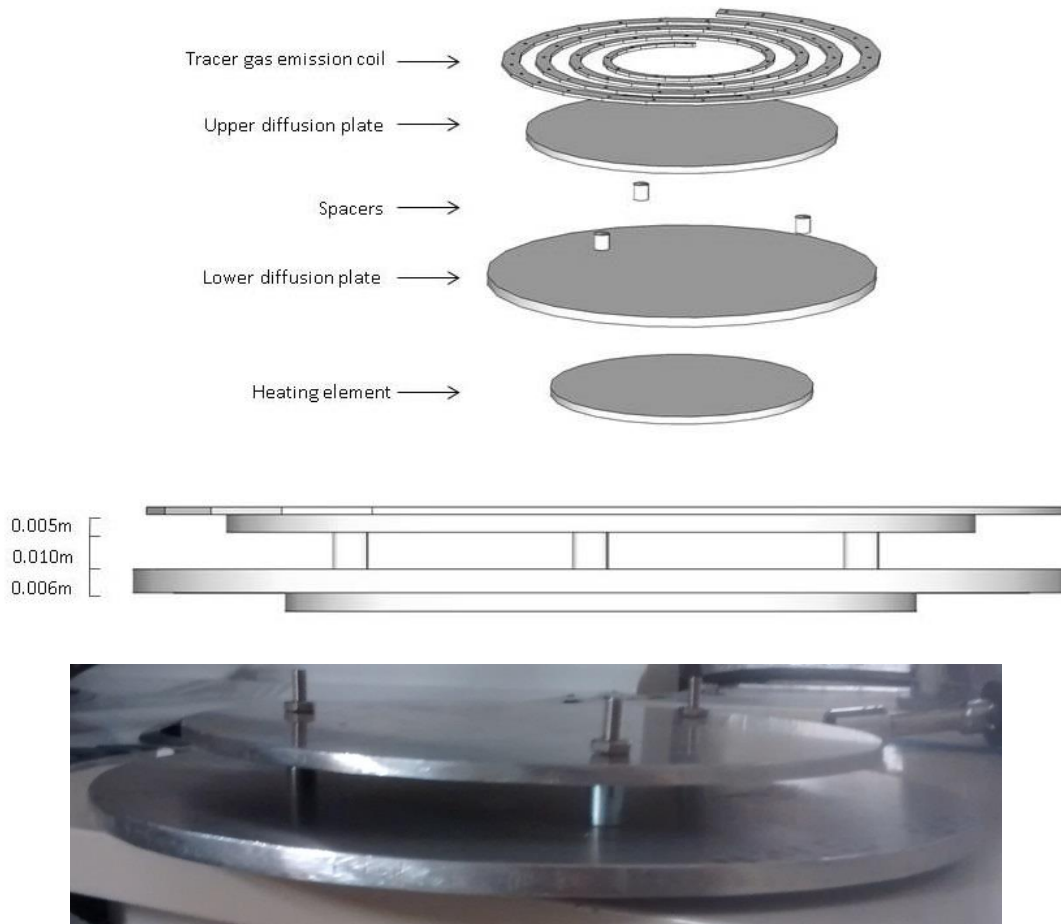


Figure 9: Example design of machined plate to be used in future experiments.

Having eliminated extreme locations and identified a reference location in the preliminary testing, subsequent tests were focused on evaluating the uncertainty associated with using this single reference point. Nine other chamber sampling locations (shown in blue in in Figure 10), were used to determine the spatial variation of the chamber concentration and the uncertainty introduced by calculating capture efficiency using a single chamber sampling location instead of an average of multiple locations.

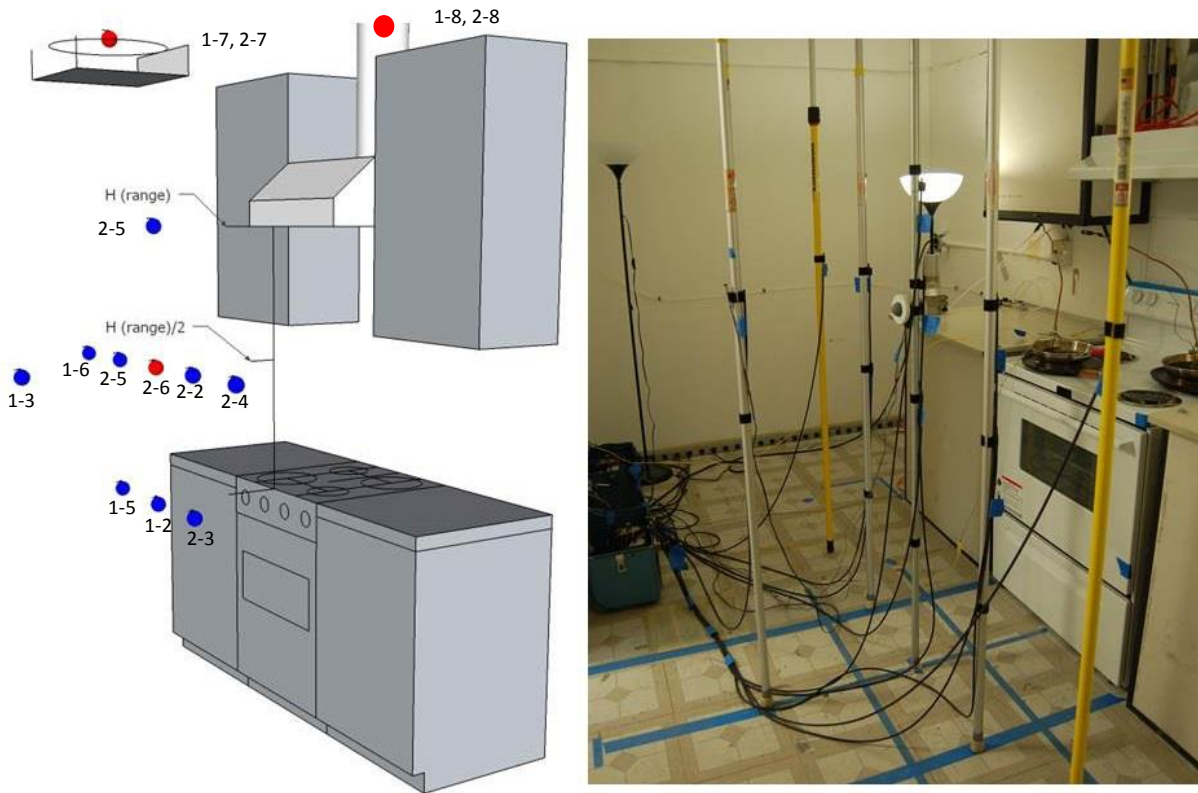


Figure 10 Sketch and photograph of central and supplemental chamber sampling locations

We used two CO₂ analyzers, each connected to a multi-port valve so that multiple locations could be sampled by each analyzer. Figure 10 shows the sampling locations that correspond to each of the ports for each of the tracer gas analyzers. The sampling ports are labeled with the first number corresponding to the analyzer and the second number the location within the test chamber. Except for port 1-3, they are located in the plane 0.5m from the front of the range. Port 1-3 is centered horizontally and vertically equidistant from the top of the cooktop and bottom of the range hood, but located 1 meter away from the front of the cooktop (instead of 0.5 m). Port 2-6 – centered in front of the cooktop and 0.5 m away and at a height equidistant from the cooktop and bottom of the range hood – is the reference room sampling location. The average concentration of locations 1-4, 1-2, 2-6, 2-5, 2-3, and 2-2 – 2-6 and the ports orthogonal to 2-6 – represent the central “cross” concentration. The cross concentration is assumed to represent the concentration of tracer gas in air entering the plume.

The two CO₂ analyzers used were PP Systems SBA-5s. There are seven ports for each analyzer, numbered 2 through 8. Ports 2 through 6 for each analyzer are test chamber sampling locations. Port 7 for both analyzers is sampled at the chamber inlet, representing the ambient CO₂ concentration. Port 8 for both analyzers is sampled in the exhaust stream downstream of the range hood and upstream of the inline flow meter. Multi-position Valco valves with programmable controllers were used to select the sampling locations for the analyzers. An auxiliary pump was added to the outlet line of the analyzers. It ran at 3.7 liters per minute divided equally between the two analyzers. The purpose for the auxiliary pump was to supplement the analyzers’ internal pumps to reduce the response time for the sampling. The analyzer line exhausted into the monitoring chamber.

The tracer gas flow rate was changed for each test in order to keep the exhaust concentration within the calibrated range of the CO₂ analyzers, which in our case is 1000 - 3500 ppm (the low limit is set by the need to resolve changes about background CO₂ levels and the upper limit was based on the highest concentrations used in calibration of the CO₂ sensors. For our test chamber and the range hood flows we studied, the tracer gas flow rate was typically between 7 and 11 liters per minute.

Each of the valve controllers was programmed to cycle through its 7 valve port locations, switching to the next location every 40 seconds such that each location is sampled every 280 seconds. The CO₂ analyzers take a measurement every 1.6 seconds. Thus, each port location is measured 25 times within each 40 second period. The first 10 measurements are discarded because they may contain air from the previous sampling location. This leaves approximately 15 measurements from each location for each 40 second sampling interval.

The duplicate inlet and exhaust concentrations from the two CO₂ analyzers were averaged together and used as the representative concentrations for the inlet and exhaust locations. In production testing, a single analyzer is recommended for the exhaust, inlet, and chamber concentrations in order to minimize uncertainty due to differences in calibration between CO₂ analyzers.

The pan surface temperatures were measured by magnetic surface-mount thermocouples and monitored using a Fluke 52-2 thermometer. Chamber temperature was kept between 15 and 30 degrees C in order to maintain conditions comparable to a residential kitchen and to avoid adversely affecting temperature-difference-driven dynamics of the heat plume generated by the cooktop.

To investigate the potential uncertainties arising from changes in test chamber air temperature we can use the fundamental relationships between plume size and temperature. The size of the plume (volumetric flow rate) at a certain height is proportional to the cube root of the input power to the plume¹ (Awbi, 1991) based on the summary provided by Chen and Rodi, 1980). The input power will be the convective heat transfer coming off of the top of the heated surface, and is directly proportional to the temperature difference between the surface and the surrounding temperature. Therefore the size of the plume is proportional to the cube root of the temperature difference between the surface and the room. Figure 11 shows how this varies with varying test chamber temperatures. The size of the plume likely varied by $\pm 1\%$ over the range of temperatures encountered in this study. To limit the uncertainties due to this variable it is recommended that chamber temperatures be maintained within a 15 to 30 °C range.

¹ Note that this is not the same as the power input to the electric element because some of that electrical power is radiated and not convected from the hot surface. As the element temperature increases the fraction of power due to radiation increases. This is one reason for avoiding extreme temperatures during these capture efficiency tests. Kosonen et al. (2006) give more details on this topic.

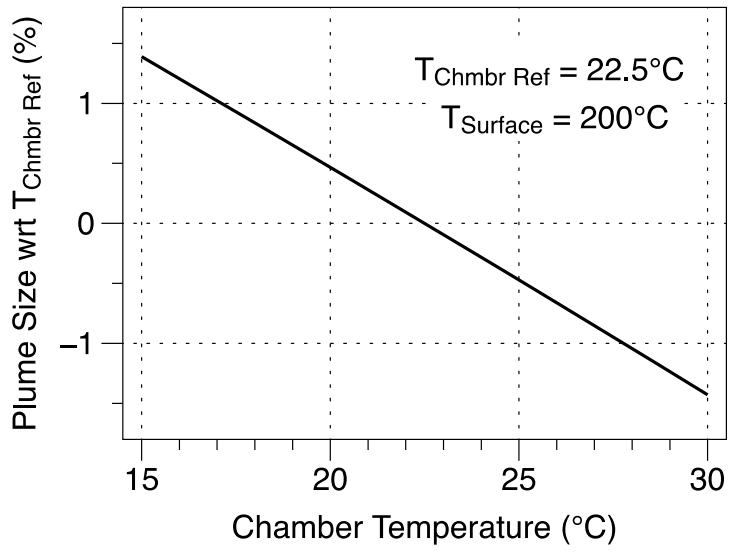


Figure 11. Variation plume size with test chamber air temperature

IV. Procedure

The following step-by-step procedure was used for each test.

1. Adjust range hood position to target height above cooktop.
2. Start laptop software to measure airflow, CO₂, and cooktop power.
3. Turn on thermometer to monitor cooktop surface temperature.
4. Turn on electric elements to begin to get pans up to the target temperature of 200 degrees C.
5. Turn on range hood and adjust range hood setting, inline fan, and iris damper to achieve target air flow for the test.
6. Ensure that the test chamber door and other chamber access points are closed.
7. Once surface temperature for both pans has stabilized to 200 degrees C (± 5 degrees), target airflow is achieved, and all monitors are logging properly, open the valve to release CO₂ tracer gas into the tracer gas emitter. Use the mass flow controller to maintain 1000-3500 ppm in the range hood exhaust.
8. Once the chamber, exhaust, and inlet concentrations have reached steady-state, the test period is considered to have begun. Steady-state was assumed to have been achieved when differences between chamber concentration (C_c) between two consecutive time samples (taken five minutes apart) was less than 5% of C_c from the second time sample. This steady state condition is generally achieved once the chamber has undergone four air changes. Air changes are calculated by dividing the volumetric air flow rate of the exhaust flow by the chamber volume.
9. Record the tracer gas concentrations in the incoming air stream (C_i), the test chamber (C_c) and exhaust (C_e) for at least 10 minutes.

If there is another target airflow to be tested start the testing at step 5.

10. Average the tracer gas concentrations and calculate the CE using these average values in Equation 1.

For step 8, there is a requirement that must be met when determining if steady state had been reached. The following method was used to determine the variability over a five minute period. The following procedures are specific to the multi-point sampling technique that we used. For production testing this could be significantly simplified. Each analyzer cycled through 7 locations, with 40 seconds of measuring at each location such that each location was sampled every 280 seconds. This cycle was repeated several times until steady-state conditions were achieved. The cycling continued after steady state for selected tests in order to examine repeatability uncertainty. To examine data that were 5 minutes apart, we compared data that overlapped inside a five-minute time window². For our data, the last five measurements from the sample in the first cycle were compared to the first five measurements (after discarding the first ten) from the second cycle for the same location. The difference between these two measurements was divided by the exhaust concentration from the second cycle. If this ratio was less

² Note that this is not strictly necessary. It would have been simpler to say that 280 seconds is close enough to five minutes and use the whole sample rather than five points from the beginning of one sample and five points from the end of another.

than 5% - then steady state was assumed. Subsequent analysis of the test results has indicated that this approach was problematic due to the gaps in time between samples for a given location and variability in exhaust gas concentrations with time. Therefore we will later consider an alternative approach that is based on the number of air changes in the test chamber provided by the range hood that is both simpler to follow and is based on fundamental conservation of mass calculations.

For step 10 we analyzed the tracer gas concentrations in several ways. The first was to use the single reference location in the chamber. We also averaged the tracer gas concentration for all the other chamber sampling locations. These additional measurements were used to develop uncertainty estimates arising from using the single reference location. For some tests, after steady state was reached the cycling through the sampling locations was repeated several times. This allowed the estimation of repeatability uncertainty. To save time when testing a range hood at multiple air flow rates, we did not reset the experiment and wait for steady state for each flow rate. Instead, after the initial wait for steady state, and the recording of data for the first tested flow rate, we continued to inject tracer gas and recording data as the flow rate was changed. There were slight delays in waiting for the new steady state condition at the higher or lower air flow rate to be reached, but these are less than what starting from scratch.

V. Results

In total eight range hood models were tested and twenty seven unique model-height-flow-rate combinations were tested. Summary characteristics of the range hoods are given in Appendix A.

Over 43,000 carbon dioxide measurements were made, and over 17,000 of those measurements were made under steady state conditions. In the test chamber, the minimum tracer gas concentration was 461 ppm of carbon dioxide, the maximum was 2275 ppm, and the median was 742 ppm. At the inlet, the minimum was 431 ppm, the maximum was 661 ppm, and the median was 482 ppm. In the exhaust stream, the minimum was 1113 ppm, the maximum was 3809 ppm, and the median was 2429 ppm.

The relative humidity measured in the chamber ranged from 33% to 63% across all the tests. As the chamber temperature rises in the course of the test, the relative humidity decreases. The decrease in relative humidity during the course of the test ranged from 6-18%.

The measured exhaust airflow rates across all the steady state tests ranged from a low of 78 cfm to a high of 444 cfm. The median airflow was 202 cfm.

The maximum measured duct pressure relative to ambient was 338 Pa, the median for all tests was 69 Pa. This pressure was measured at the flow nozzle used to monitor the airflow. This nozzle is downstream of the range hood, but upstream of both the in-line supplemental fan and the iris damper at the outlet. The relative contribution of the two fans and the restriction setting of the iris damper all affected the duct pressure. These pressures were used to correct the measured flow from the flowmeter for any duct leakage between the flow meter and the range hood.

The averaged pan surface temperature during the tests was 200 ± 5 degrees C, but the momentary measured temperatures during the tests ranged from 185-212 degrees.

VI. Analysis

Reaching steady state conditions

Our criterion for steady state is the ratio of the changes from one sample cycle to the next (roughly over a five minute time period) to C_{exhaust} . We also looked at the change in CE calculated for every sample cycle (using the same concentration) data to see if CE and the concentrations reached steady conditions at the same time. Because the time to reach steady state also depends on the chamber volume and the air flow through the chamber, we examined the results in terms of chamber air changes. In Figure 12, the change in concentrations and the change of capture efficiency are plotted against the number of air changes the chamber has undergone since the release of the tracer gas. The red line represents the 5% threshold set for steady state concentrations. Time zero is when the tracer gas was first released into the chamber (pan temperature and range hood airflow were already stabilized by time zero).

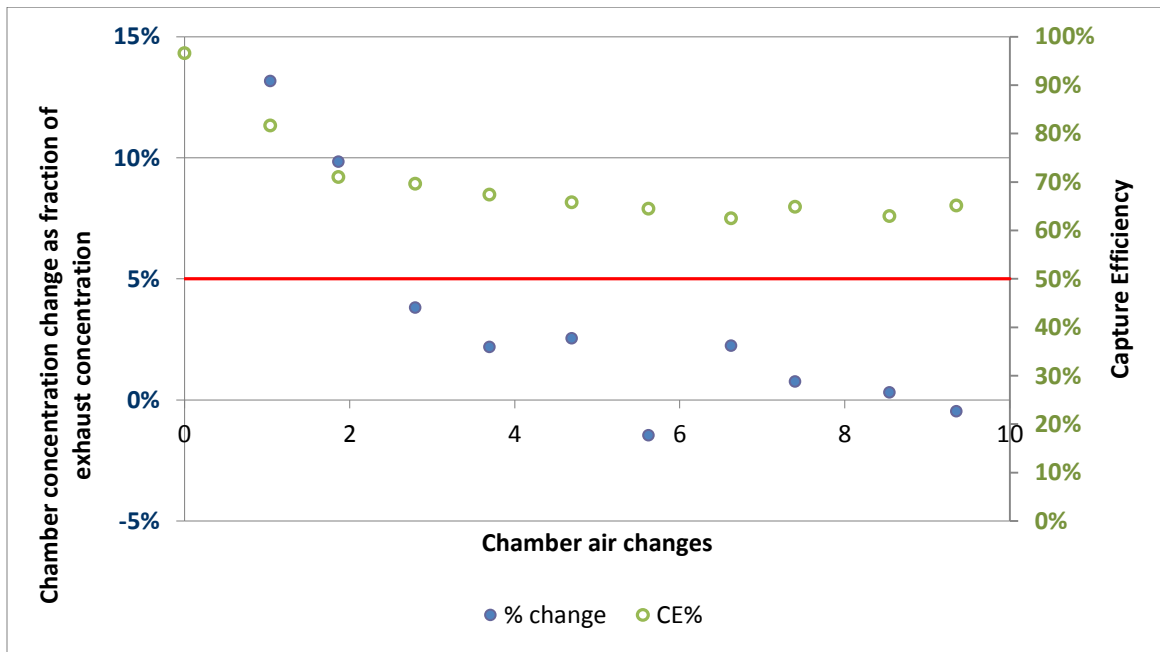


Figure 12: QP130WW Stabilization of capture efficiency and tracer gas concentration in terms of chamber air changes.

In the test of the QP130WW range hood, shown in Figure 12, the first measurement below the 5% threshold was at just under 3 chamber air changes. All subsequent measurements are below this 5% threshold and are considered to be occurring under steady state conditions. The CE has also reached steady state by this point.

Figure 13 and Figure 14 depict the same process of reaching steady state conditions in more detail for a different test using a microwave range hood³. In addition to the tracer gas percent change and CE, Figure 13 also shows the tracer gas concentrations (in ppm) in the chamber, at the inlet, and in the outlet stream. These results show that it takes several chamber air changes for concentrations to reach steady-state. For the same test, Figure 14 shows the range hood airflow and the chamber temperature at the reference sampling location, both facing toward the cooktop and facing away from the cooktop (left y-axis). The average cooktop power is plotted against the right y-axis. The cooktop temperature remained constant at 200 ± 5 degrees C, but the chamber temperature gradually increased during the

³ Commonly referred to as over-the-range (OTR) microwave ovens.

course of the testing. The power input into the cooktop remained stable – around 2 kW – during the course of the experiment. The range hood airflow ranged between 136.5-140.5 cfm during the test.

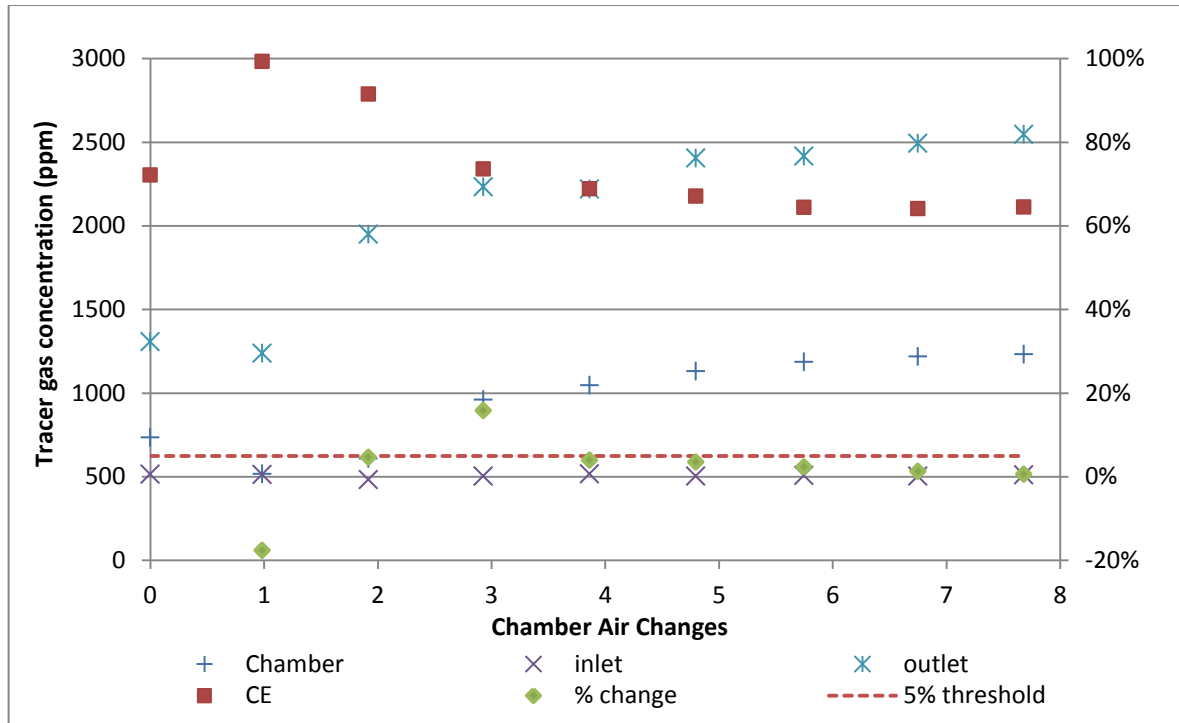


Figure 13: Panasonic NNDS277SR, 36-inch height. Concentration changes vs. capture efficiency, by chamber air changes.

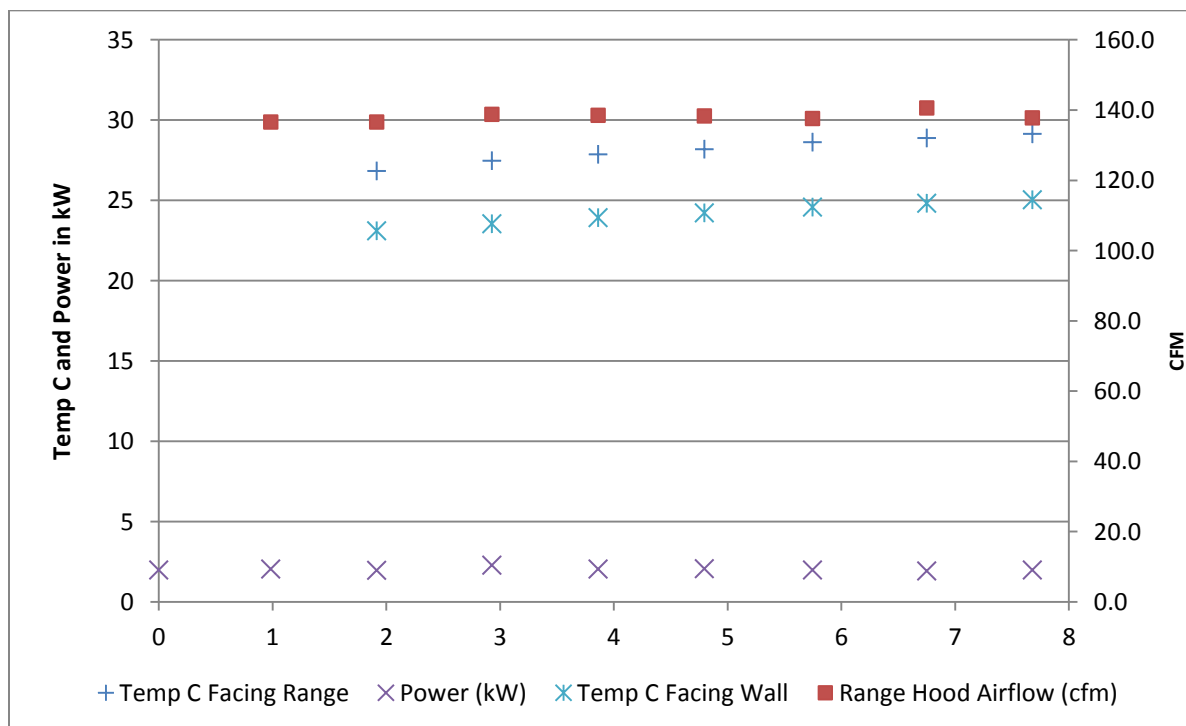


Figure 14: Panasonic NNDS277SR, 36-inch height. Chamber temperature, cooktop power, and range hood airflow, by chamber air changes.

For the microwave range hood test, the 5% change steady state threshold occurred between 3 and 4 air changes.

The number of elapsed air changes before reaching steady state (using the 5% change criterion) was calculated for all range-hood/mount-height/flow-rate combinations tested. The results are shown in Table 2. On average 3.3 air changes were needed to reach steady-state using this approach.

These steady state air change numbers vary across the test conditions, with no clear pattern with relation to model, mounting height, or airflow. Based on these findings, 8 air changes are necessary to ensure that steady state conditions have been reached for all tests. However, in most cases 4 air changes is sufficient. Detailed analysis of the test results indicated that some of the variability in these results was due to a combination of time-variation of exhaust air tracer gas concentrations and the significant time gaps between samples. Therefore we suggest that the following, more fundamental approach be used in future testing.

Table 2: Chamber Air Changes Required to reach Steady State Conditions.

Manufacturer	Model	Height (in)	Height (cm)	Airflow (CFM)	Airflow (L/s)	Air Changes
Air King	ESDQ1303	20	51	265	125	2.9
Air King	ESDQ1303	20	51	266	126	2.9
Air King	ESDQ1303	29	74	141	67	2.2
Air King	ESDQ1303	29	74	146	69	2.1
Broan	403001	24	61	86	41	5.5
Broan	403001	24	61	107	51	1.5
Broan	403001	24	61	225	106	3.2
Broan	403001	30	76	160	76	8
Broan	403001	30	76	162	76	8.1
Broan	CBD130SS	18	46	110	52	5
Broan	CBD130SS	18	46	111	52	3.1
Broan	CBD130SS	18	46	146	69	4.1
Broan	CBD130SS	24	61	110	52	1.4
Broan	CBD130SS	24	61	150	71	1.9
Broan	CBD130SS	24	61	151	71	1.9
Broan	QP130WW	24	61	110	52	1.4
Broan	QP130WW	24	61	302	143	3.3
Broan	QP130WW	30	76	112	53	2.5
Cavaliere	AP238PS6330	26	66	192	91	2.7
Cavaliere	AP238PS6330	26	66	203	96	3.2
Cavaliere	AP238PS6330	26	66	297	140	4.2
Panasonic	NNSD277SR	30	76	137	65	3.9
Panasonic	NNSD277SR	30	76	303	143	5.7
Panasonic	NNSD277SR	36	91	138	65	1.9
Panasonic	NNSD277SR	36	91	208	98	4.5
Sakura	U2F	24	61	155	73	1.9
Sakura	U2F	24	61	199	94	2.5
Sakura	U2F	24	61	306	144	0.5
Sakura	U2F	24	61	437	206	4.8
Sakura	U2F	31	79	147	69	2.5
Sakura	U2F	31	79	152	72	2.4
Sakura	U2F	31	79	199	94	3.1
Vent-a-Hood	B100	24	61	231	109	5.4
Vent-a-Hood	B100	24	61	295	139	3.2
Vent-a-Hood	B100	24	61	295	139	3.2
Vent-a-Hood	B100	24	61	295	139	3.2
Vent-a-Hood	B100	28	71	232	110	4.7
Vent-a-Hood	B100	28	71	281	133	4.4
Vent-a-Hood	B100	28	71	296	140	3.2

Mass Balance Approach

If we assume that the chamber is well mixed we can theoretically calculate the bias errors introduced by not waiting until steady state. The concentration in the chamber changes with time as a function of the tracer gas injection rate, the capture efficiency of the range hood and the air flow rate through the test chamber (the range hood exhaust rate), and can be expressed as:

$$C_c = (1 - \eta) \frac{S}{Q} (1 - e^{-\lambda t})$$

where:

η is the true capture efficiency

S is the tracer gas release rate (kg/s)

Q is the flowrate through the hood (kg/s)

λ is the ventilation rate of the chamber (at the hood flowrate) normalized by chamber volume

t is time from the start of a test (turning on the tracer gas)

The concentration in the exhaust will be what is captured by the hood plus the concentration in the room:

$$C_e = \eta \frac{S}{Q} + C_c$$

The steady state formulation for capture efficiency is

$$CE = \frac{C_e - C_c}{C_e - C_i}$$

If we assume $C_i = 0$ we get the apparent CE as a function of the true efficiency and time

$$CE = \frac{\eta}{\eta + (1 - \eta)(1 - e^{-\lambda t})}$$

The bias would be this apparent CE minus the actual efficiency (η), and this is shown in Figure 15. The product of λ and t is the number of air changes, and is a way of expressing the time. The bias is positive if the concentrations are growing in the chamber, and negative if falling. The bias is larger with lower capture efficiencies, at 2 room changes the bias is slightly over 2% for a CE of 80% but is over 3% with CEs lower than 60%. The bias is below $\pm 0.5\%$ at points in time exceeding 4 air changes, therefore we recommend waiting for 4 air changes for steady-state testing. In some situations this requirement may be shorter. For example, if there is a short time between consecutive tests, then the tracer concentration in the room will start nearer steady state than if starting from zero concentration. However, for consistency in a standardized test procedure we recommend always using the 4 air changes criteria.

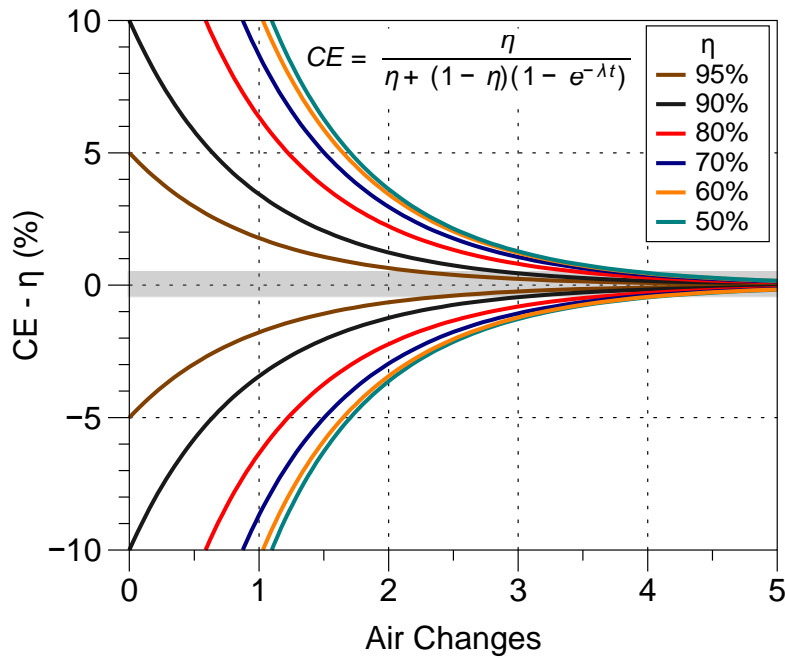


Figure 15. Capture Efficiency errors due to not being at steady state

Reducing Sampling Strategy Errors

We measured considerable variability in the exhaust tracer gas concentrations compared to the room and inlet due to plume intermittency and lack of perfect mixing. To examine this further, a test was performed without switching between all sampling locations such that the time resolution was significantly enhanced. Figure 16 shows the resulting tracer gas measurements.

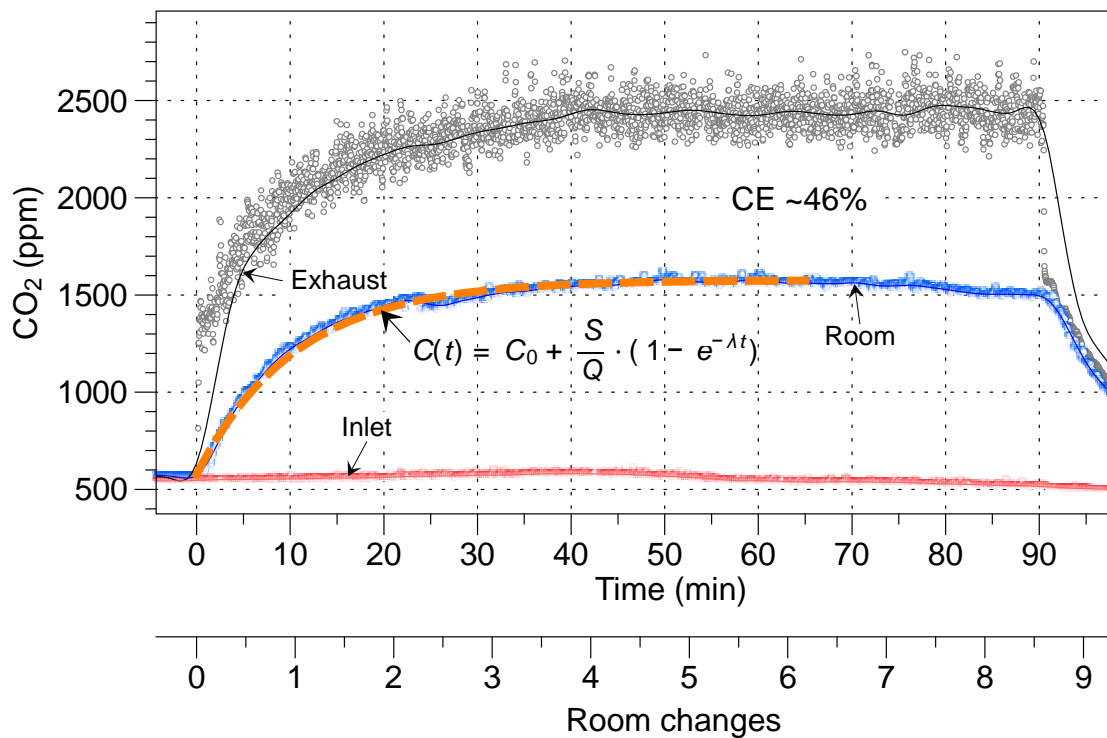


Figure 16. Time Evolution and Variability in and Room Exhaust Concentrations

It looks like the experiment is close to steady state after 4 room changes, but there is considerable short-term variability in the exhaust measurements. The data shown represents data taken roughly every 1.6 s (there are gaps due to instrument auto-zeros). These results imply that the experimental procedure needs to specify the number of sampling points and/or how long to sample for.

Figure 17 shows the individual measurements together with a 30 s running average. The green dots are representing points that would result from a 5 min sampling scheme we employed with the testing (the multiplexing came back around after ~5 min, and each stop represented ~30 s of data). These results show that the differences between successive 5 min samples, or different 5 min windows could lead to successive measurements being closer together or further apart than the criteria we used, leading to falsely long or short times to reach steady-state. This explains the variability in the results shown in Table 2.

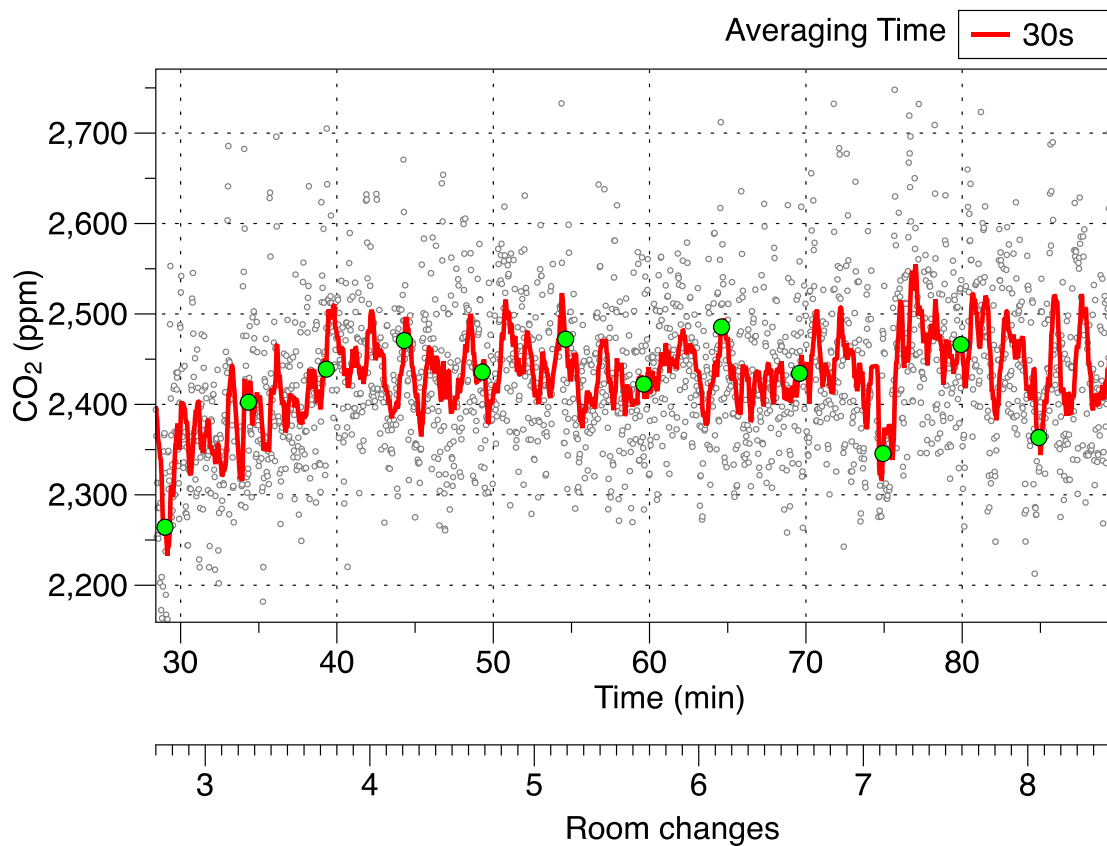


Figure 17. Effect of time averaging and periodic sampling of exhaust tracer gas concentrations

Figure 18 shows both the exhaust numbers and the corresponding relative standard error in the means for a given sampling period. Even with 30 s averaging the RSE of the mean is usually less than 1%. This tells us that regardless of the averaging period each point is well known.

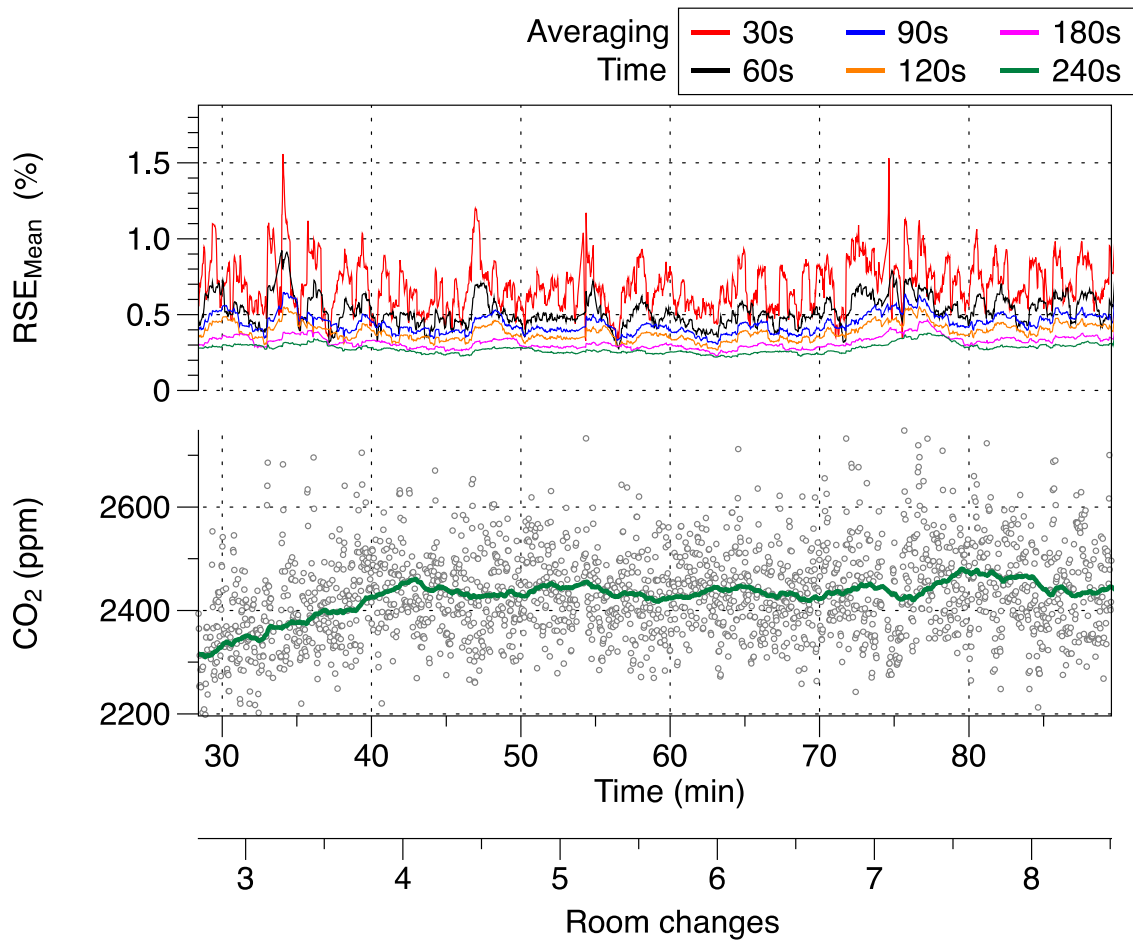


Figure 18. Effect of averaging time on error in the mean for exhaust concentrations

Figure 19 shows the exhaust data using different averaging times. Even well beyond the 4 room changes there is variability in the running averages in exhaust stream. Using a four-minute average smooths out much, but not all of the fluctuations.

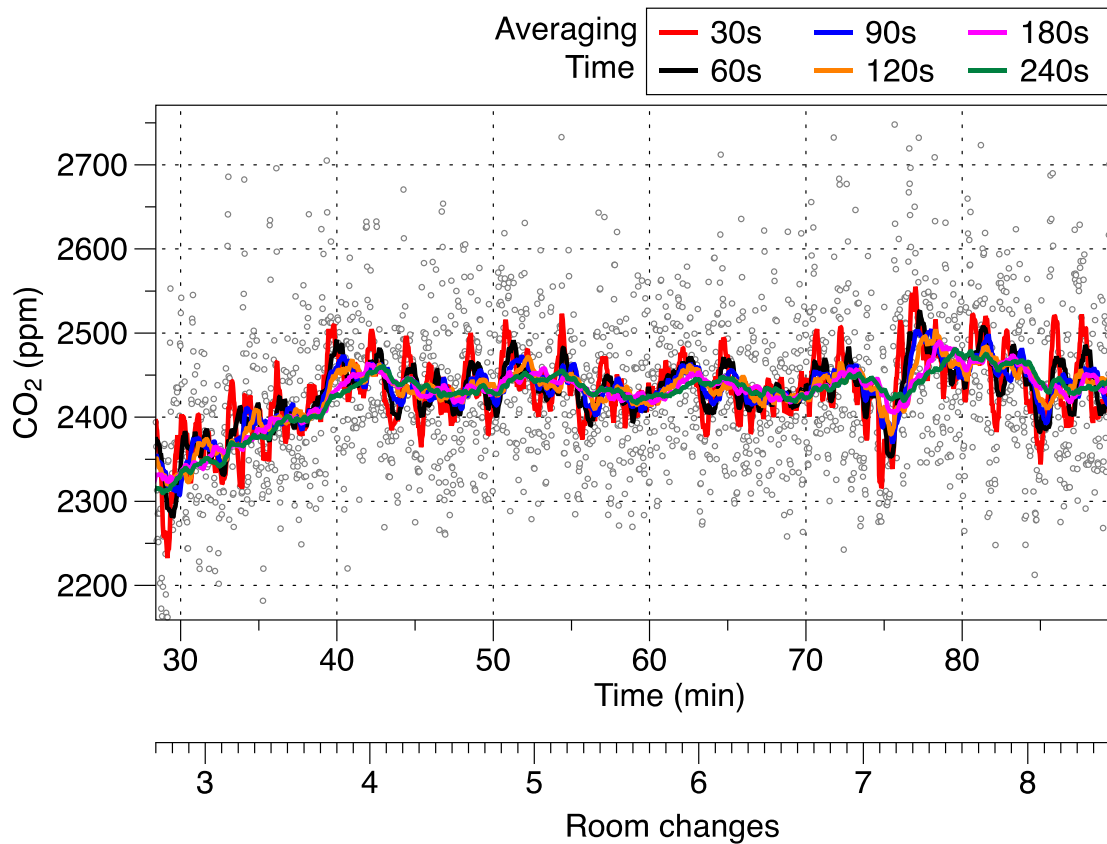


Figure 19. Effect of averaging time on exhaust concentrations

To further investigate the time averaging requirements, capture efficiency was calculated using 30s, 4 minutes and 10 minute averaging periods and compared to the long term average (LTA) capture efficiency over about 55 minutes. Figure 20 shows the possible errors using different averaging periods. The bottom panel is the running CE (using the stated averaging period), and the top panel is this CE minus the CE calculated using the LTA. With the 4 or 10 minute data the majority of results lie within $\pm 1\%$ of the LTA value. Even with the 30 s values the median is the same as the LTA, we just may get values that are $\pm 4\%$ of the LTA. The reason for the long period changes in CE are currently unknown. Analysis of the exhaust fan airflow indicated that air flows did not change during this testing period. It is possible that there are fluctuations in tracer injection rate for some reason, but we were not able to definitively determine if that is the case.

The results of the more in-depth analysis of signal averaging requirements indicate that the sampling room should be run for a minimum of 4 room changes before taking any data used in the capture efficiency calculations. The tracer gas concentrations should be averaged for at least 5 minutes.

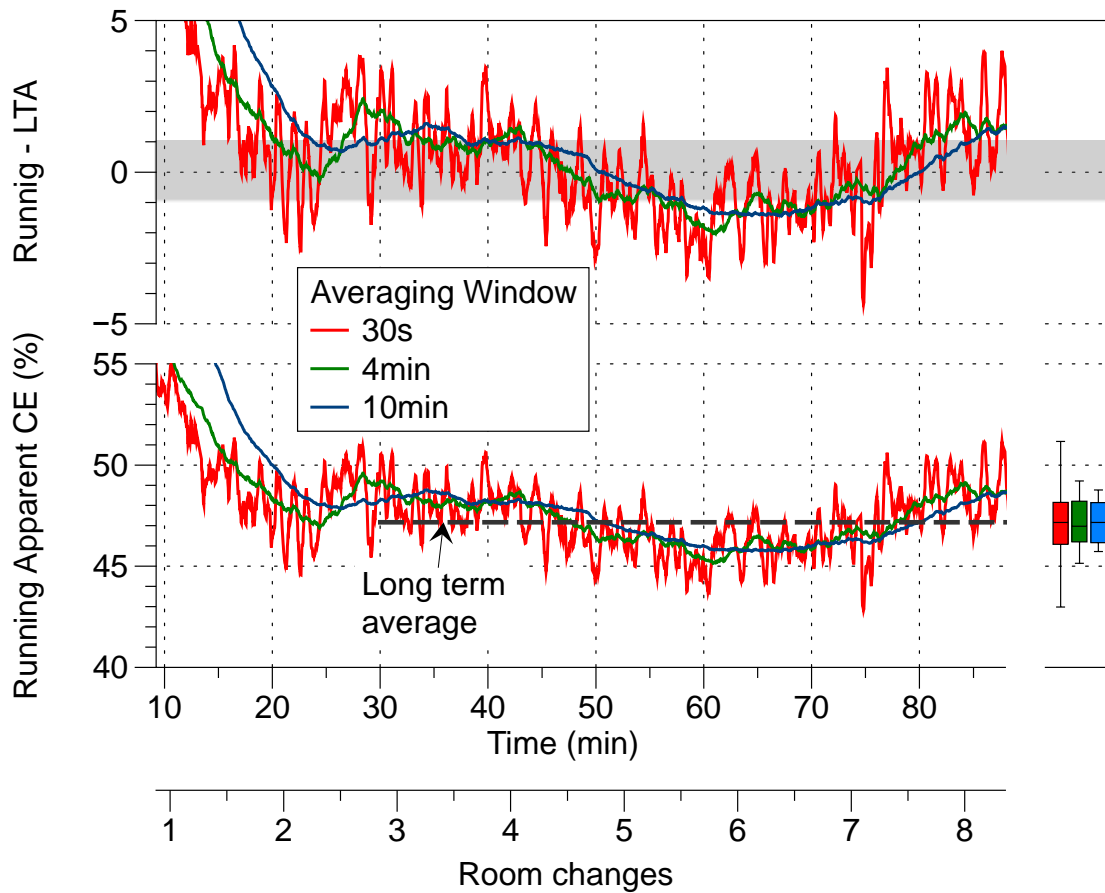


Figure 20. Comparing long term and short term averaging capture efficiencies

Uncertainty

Two kinds of error contribute to the uncertainty of the range hood capture efficiency measurements: precision error that is a combination of the accuracy of the tracer gas analyzer and spatial variations in concentration, and temporal error (the uncertainty due to fluctuations in tracer gas concentration). The accuracy of the tracer gas analyzer is +/- 1%. This uncertainty is present in all the tracer gas measurements but does not propagate into the error in CE due to the calculation being a ratio of differences such that absolute biases are removed by taking differences between two concentrations and fractional errors because CE is the ratio of two concentrations. Note that this is strictly only true if the same analyzer is used for all concentration measurements, or, if two or more analyzers are used, they have the same inaccuracy. In our experiments, the analyzers were cross calibrated so we are able to assume that this basic analyzer inaccuracy can be ignored.

Precision error

The spatial error arises from non-representative measurements because the tracer gas is not spatially uniform. It is calculated for all three tracer gas measurement locations: in the exhaust stream ($C_{exhaust}$), in the test chamber ($C_{chamber}$), and in the inlet stream (C_{inlet}). The spatial errors for these measurements are designated by $\delta_p(C_{exhaust})$, $\delta_p(C_{chamber})$, and $\delta_p(C_{inlet})$.

$$\delta_p(C_{exhaust})$$

$\delta_p(C_{exhaust})$ accounts for the spatial variation of the tracer gas concentration in the exhaust stream. The 20 cm-diameter exhaust ducting was sampled using a cross-sectional array with 5 points spaced 5 cm apart. This array was installed 12 effective diameters downstream of the range hood. This combination of multiple sample locations and distance from the range hood meet the requirements of ASTM E2029 (2004) for measuring tracer gases in ducts. Therefore we assume an effective error of zero.

$\delta_p(C_{chamber})$

$\delta_p(C_{chamber})$ accounts for the spatial variation of the tracer gas concentration in the test chamber. Ten locations were sampled within the test chamber to characterize the variation throughout the chamber. The locations furthest from the range hood were used to qualitatively examine air flow patterns within the room. Five points were selected that were in front of the range hood and would not experience any large-scale recirculation of any meandering plume not captured by the range hood. They are also located where anyone doing any cooking is likely to be and could be thought of as representative of air being breathed by a cook (although it is not the intent to evaluate a cook's exposure to cooking pollutants directly). The chamber concentration is intended to characterize the concentration of air from the room that is captured by the range hood before any tracer is added by the plume above the heater elements. The uncertainty associated with selecting a single sample location rather than spatially averaging over all five locations is given by $\delta_p(C_{chamber})$ and was calculated by taking the root mean square (RMS) of the difference between each tracer gas concentration measured at the center point and the average of the five "cross" location concentrations, all measured during the same 5-minute period.

$\delta_p(C_{inlet})$

$\delta_p(C_{inlet})$ accounts for the spatial variation of the tracer gas concentration in the inlet stream. The inlet stream is from well-mixed ambient sources so $\delta_p(C_{inlet})$ was assumed to be zero.

Temporal error

The temporal variation of the tracer gas measurements is indicated by the standard error of the mean (SEM) concentration values for each 15 point sample. The SEM is calculated by dividing the standard deviation of the data set by the square root of the sample size. These variations are expressed as $\delta_{se}(C_{exhaust})$, $\delta_{se}(C_{chamber})$, and $\delta_{se}(C_{inlet})$.

Total error

Total error of the concentrations are expressed as $\delta(C_{exhaust})$, $\delta(C_{chamber})$, and $\delta(C_{inlet})$, and calculated as follows:

$$\delta(C_{exhaust}) = \sqrt{(\delta_p(C_{exhaust}))^2 + (\delta_{se}(C_{exhaust}))^2}$$

Equation 2

$$\delta(C_{chamber}) = \sqrt{(\delta_p(C_{chamber}))^2 + (\delta_{se}(C_{chamber}))^2}$$

Equation 3

$$\delta(C_{inlet}) = \sqrt{(\delta_p(C_{inlet}))^2 + (\delta_{se}(C_{inlet}))^2}$$

Equation 4

Total error in capture efficiency (δCE) is calculated as:

$$\delta CE = CE \left[\sqrt{\frac{(\delta(C_{exhaust}))^2 + (\delta(C_{chamber}))^2}{(C_{exhaust} - C_{chamber})^2} + \frac{(\delta(C_{exhaust}))^2 + (\delta(C_{inlet}))^2}{(C_{exhaust} - C_{inlet})^2}} \right]$$

Equation 5

Example calculation

The following example calculation was made using actual test data from a test of the Broan model QP130WW range hood mounted 24 inches above the cooktop and with an air flow of 110 cfm.

Precision Error

$$\delta_p(C_{exhaust})$$

Because in this experiment $C_{exhaust}$ was measured 12 effective downstream diameters from the range hood using a five-point array across the duct, we presume $\delta_p(C_{exhaust})$ to be zero.

$$\delta_p(C_{chamber})$$

The center point concentration was 1186 parts per million (ppm) of carbon dioxide, and the concentrations at the other four locations were 1191, 1206, 1218, and 1195 ppm. The average of the five points is 1199 ppm, and the difference between this average and the concentration at the single center point is $1186 - 1199 = -13$ ppm. This value is the difference for a single sampling period.

This same difference is calculated for every steady-state sampling period available for each test and the RMS of all the differences calculated. For this example test, there were six steady-state measurements, and the differences were -13, 16, -3, 19, -2, 29, and 17 ppm. The RMS of these differences is 16 ppm.

i.e., $\delta_p(C_{chamber}) = 16$ ppm.

$$\delta_p(C_{inlet})$$

Because in this experiment C_{inlet} was measured from a well-mixed ambient source, $\delta_p(C_{inlet})$ is presumed to be zero.

Temporal Error

The SEM was calculated for all exhaust concentration measurements taken within a single five-minute sampling period. For the example test, we completed multiple five-minute sampling periods, and then averaged the SEMs for all the periods for each location. The values were as follows:

$$\delta_{se}(C_{exhaust}) = 27.2 \text{ ppm}$$

$$\delta_{se}(C_{chamber}) = 16.4 \text{ ppm}$$

$$\delta_{se}(C_{inlet}) = 6.8 \text{ ppm}$$

Total Error

$$C_{exhaust} = 2758, \delta_p(C_{exhaust}) = 0, \delta_{se}(C_{exhaust}) = 27.2$$

$$C_{chamber} = 1133, \delta_p(C_{chamber}) = 16.4, \delta_{se}(C_{chamber}) = 2.4$$

$$C_{inlet} = 483, \delta_p(C_{inlet}) = 0, \delta_{se}(C_{inlet}) = 6.8$$

$$CE = \frac{C_e - C_c}{C_e - C_i} = \frac{2528 - 1133}{2528 - 483} = 0.64$$

$$\delta(C_{exhaust}) = \sqrt{(\delta_p(C_{exhaust}))^2 + (\delta_{se}(C_{exhaust}))^2} = \sqrt{0^2 + 27.2^2} = 27.2$$

$$\delta(C_{chamber}) = \sqrt{(\delta_p(C_{chamber}))^2 + (\delta_{se}(C_{chamber}))^2} = \sqrt{16.4^2 + 2.4^2} = 16.6$$

$$\delta(C_{inlet}) = \sqrt{(\delta_p(C_{inlet}))^2 + (\delta_{se}(C_{inlet}))^2} = \sqrt{0^2 + 6.8^2} = 6.8$$

$$\delta CE = CE \left[\sqrt{\frac{(\delta(C_{exhaust}))^2 + (\delta(C_{chamber}))^2}{(C_{exhaust} - C_{chamber})^2} + \frac{(\delta(C_{exhaust}))^2 + (\delta(C_{inlet}))^2}{(C_{exhaust} - C_{inlet})^2}} \right] =$$

$$0.64 \left[\sqrt{\frac{(27.2)^2 + (16.6)^2}{(2758 - 1133)^2} + \frac{(27.2)^2 + (6.8)^2}{(2758 - 483)^2}} \right] = 0.64[0.027] = 0.017$$

The CE for this example test is 0.64 ± 0.017 .

Uncertainty from using a single chamber point instead of multiple points

To measure the chamber tracer gas concentration, a single point or a combination of samples from multiple locations can be used. We presume that averaging a sample of the four points orthogonal to the central “2-6” point as well as the 2-6 point is closer to the “true” chamber concentration than sampling at the central 2-6 point alone. To get an indication of the penalty associated with sampling the chamber at a single point versus multiple points, we calculated the CEs for each test using the single point and the multiple “cross” points as the chamber concentration and compared the results in Table 3. Results from several hoods are not shown in these tables because the investigation into steady-state performance indicated that the tests were not at steady state.

Table 3: Capture Efficiency sampling chamber at 1 point versus 5 points (part 1)

						CE using chamber sampling location	
Manuf.	model	Height (in)	Height (cm)	Air Flow (cfm)	Air Flow (L/s)	center (1 point)	cross (5 points)
Air King	ESDQ1303	20	51	266	126	0.95	0.95
Air King	ESDQ1303	20	51	266	126	0.95	0.95
Air King	ESDQ1303	20	51	267	126	0.95	0.95
Air King	ESDQ1303	20	51	267	126	0.95	0.95
Air King	ESDQ1303	29	74	138	65	0.66	0.67
Air King	ESDQ1303	29	74	138	65	0.64	0.66
Air King	ESDQ1303	29	74	269	127	0.86	0.87
Air King	ESDQ1303	29	74	269	127	0.85	0.86
Broan	403001	24	61	226	107	0.87	0.87
Broan	403001	30	76	88	42	0.55	0.54
Broan	403001	30	76	115	54	0.69	0.69
Broan	403001	30	76	166	78	0.74	0.74
Broan	403001	30	76	167	79	0.75	0.75
Broan	403001	30	76	167	79	0.75	0.75
Broan	CBD130SS	18	46	109	51	0.73	0.73
Broan	CBD130SS	18	46	147	69	0.89	0.89
Broan	CBD130SS	18	46	147	69	0.88	0.88
Broan	CBD130SS	18	46	257	121	0.94	0.93
Broan	CBD130SS	18	46	257	121	0.95	0.95
Broan	CBD130SS	24	61	110	52	0.68	0.67
Broan	CBD130SS	24	61	110	52	0.68	0.68
Broan	CBD130SS	24	61	150	71	0.76	0.76
Broan	CBD130SS	24	61	255	120	0.95	0.96
Broan	CBD130SS	24	61	255	120	0.95	0.95
Broan	QP130WW	24	61	109	51	0.69	0.7
Broan	QP130WW	24	61	302	143	0.96	0.96
Broan	QP130WW	24	61	302	143	0.95	0.95
Broan	QP130WW	30	76	111	52	0.63	0.64
Broan	QP130WW	30	76	112	53	0.65	0.64
Broan	QP130WW	30	76	298	141	0.97	0.96
Broan	QP130WW	30	76	299	141	0.98	0.98
Broan	QP130WW	30	76	299	141	0.98	0.98

Table 3: Capture Efficiency sampling chamber at 1 point versus 5 points (part 2)

manuf.	model	Height (in)	Height (cm)	Air Flow (cfm)	Air Flow (L/s)	CE using chamber sampling location	
						center (1 point)	cross (5 points)
Cavaliere	AP238PS6330	26	66	134	63	0.72	0.73
Cavaliere	AP238PS6330	26	66	203	96	0.8	0.8
Cavaliere	AP238PS6330	26	66	294	139	0.92	0.92
Cavaliere	AP238PS6330	26	66	297	140	0.91	0.91
Panasonic	NNSD277SR	30	76	136	64	0.66	0.66
Panasonic	NNSD277SR	30	76	137	65	0.66	0.66
Panasonic	NNSD277SR	30	76	290	137	0.91	0.91
Panasonic	NNSD277SR	30	76	291	137	0.91	0.91
Panasonic	NNSD277SR	30	76	291	137	0.91	0.91
Panasonic	NNSD277SR	36	91	138	65	0.66	0.66
Panasonic	NNSD277SR	36	91	138	65	0.65	0.64
Panasonic	NNSD277SR	36	91	301	142	0.87	0.88
Panasonic	NNSD277SR	36	91	301	142	0.86	0.87
Sakura	U2F	24	61	149	70	0.88	0.88
Sakura	U2F	24	61	150	71	0.89	0.89
Sakura	U2F	24	61	201	95	0.92	0.93
Sakura	U2F	24	61	201	95	0.92	0.92
Sakura	U2F	24	61	306	144	0.95	0.95
Sakura	U2F	24	61	306	144	0.94	0.94
Sakura	U2F	24	61	439	207	0.98	0.98
Sakura	U2F	24	61	439	207	0.98	0.99
Sakura	U2F	24	61	440	208	0.97	0.97
Sakura	U2F	31	79	148	70	0.83	0.83
Sakura	U2F	31	79	203	96	0.88	0.88
Sakura	U2F	31	79	308	145	0.93	0.94
Sakura	U2F	31	79	309	146	0.92	0.91
Sakura	U2F	31	79	309	146	0.94	0.94

Table 3: Capture Efficiency sampling chamber at 1 point versus 5 points (part 3)

manuf.	model	height (in)	Height (cm)	Air flow (cfm)	Air Flow (l/s)	CE using chamber sampling location	
						center (1 point)	cross (5 points)
Vent-a-Hood	B100	24	61	136	64	0.87	0.87
Vent-a-Hood	B100	24	61	138	65	0.88	0.88
Vent-a-Hood	B100	24	61	179	84	0.92	0.93
Vent-a-Hood	B100	24	61	180	85	0.8	0.89
Vent-a-Hood	B100	24	61	228	108	0.96	0.96
Vent-a-Hood	B100	24	61	229	108	0.94	0.93
Vent-a-Hood	B100	24	61	229	108	0.95	0.95
Vent-a-Hood	B100	24	61	297	140	0.96	0.96
Vent-a-Hood	B100	24	61	297	140	0.97	0.97
Vent-a-Hood	B100	24	61	297	140	0.97	0.98
Vent-a-Hood	B100	28	71	229	108	0.93	0.93
Vent-a-Hood	B100	28	71	229	108	0.93	0.93
Vent-a-Hood	B100	28	71	297	140	0.95	0.95
Vent-a-Hood	B100	28	71	297	140	0.93	0.94
Vent-a-Hood	B100	28	71	297	140	0.94	0.94

The differences in calculated capture efficiency using a single point versus multiple points to measure the chamber concentration have one extreme point at 9%, but in most cases is 1% or less. For the multiple measurements at the same flow the standard deviations were 1% or less. These results show that the uncertainty due to using one central point to measure the chamber concentration appears is very small.

The standard deviation of the capture efficiencies (single point and multi point) is also calculated for all of the five-minute steady state periods for each experiment. This number gives a secondary indication of the temporal variation of the capture efficiency during the experiment.

Performance of Range Hood Models

Figure 21 shows the capture efficiency (y-axis) of each test plotted against the measured air flow rate in cubic feet per minute (x-axis) of the range hood. Each range hood model's symbols have a designated color. The triangles represent tests for which the range hood was mounted at or near the highest mounting height recommended by the manufacturer. The squares represent tests for which the range hood was mounted at or near the lowest mounting height recommended by the manufacturer⁴. The

⁴ One of the models could only be tested at a single height.

symbols for tests that were compliant with ASHRAE 62 requirements for flow rates and sound level are enlarged for emphasis⁵.

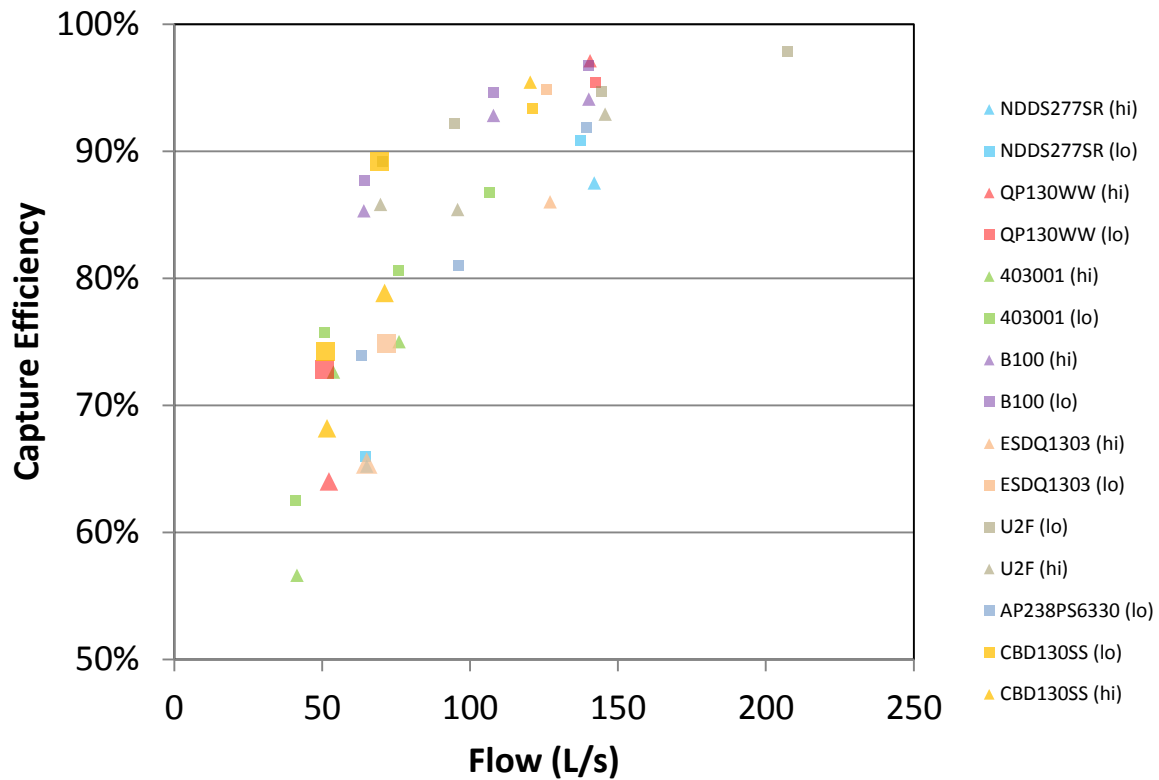


Figure 21: Capture Efficiency versus airflow for the eight range hood models tested

Figure 21 does show a general positive correlation between range hood flow rate (Q) and capture efficiency. However, there are factors other than just flow rate that determine the capture efficiency for a particular range hood. Different models have differing capture efficiencies at the same flow rate. The same range hood model at the same flow rate has differing capture efficiencies at different mounting heights. In general, all else held constant, the lower mounted range hoods (squares) had higher capture efficiencies than the higher mounted range hoods (triangles).

The difference in performance between a low-mount test and high-mount test was generally smaller for hoods with a deep sump (e.g., B100) and/or if their depth extended to cover the front burners (e.g., U2F & B100). Differences in performance -- both within tests for the same range hood (at different mounting heights) and between tests of different range hood models -- tended to decrease at higher flow rates. That is, at flow rates ≥ 300 cfm, all the range hood models has CEs exceeding 80%. However, there was significant variation in performance at flow rates less than 300 cfm.

⁵ Few of the measurements are marked with the larger symbols. Only at flows less than 150 cfm do the hoods meet 62.2's sound requirements. Of the hoods tested with flows 150 cfm or less: 403001 – HVI rated at 0.10 IWC @ 160 cfm and 6.5 sones. AP238PS6330 – not HVI rated. U2F – not HVI rated. NDDS277SR – not HVI rated (microwave). B100 – not HVI rated. The more expensive units (Cavaliere, Vent-a-Hood, Sakura) were not be HVI rated.

This is significant because mandating that all range hoods shall be installed to have flows of at least 300 cfm is not practical. Higher flows both increase the energy penalty of using a range hood and, because of noise, make it less likely that a range hood will be used. For these reasons, it is important to determine the characteristics that enable a range hood to have a sufficiently high CE at a relatively low flow rate.

Characterizing the Variability of the Tracer Gas Concentration in the Test Chamber

As described in Figure 10, ports 2 through 6 for each analyzer sample the test chamber, port 7 samples the inlet, and port 8 samples the exhaust.

Table 4: Concentrations across port sampling locations

manuf.	model	ht(in)	cfm	1-2		1-3		1-4		1-5		1-6		1-7		1-8		2-2		2-3		2-4		2-5		2-6		2-7		2-8	
				M	SEM	M	SEM	M	SEM	M	SEM	M	SEM	M	SEM	M	SEM	M	SEM	M	SEM	M	SEM								
Broan	403001	24	109	940	1.4	937	0.3	955	0.6	1079	6	960	0.8	449	0.5	2321	26.1	962	3.5	919	0.6	957	1.6	964	1	974	1.6	450	0.3	2275	31.1
Broan	403001	24	110	1993	2.9	1938	3.1	1898	1.6	1909	4.3	1780	3.4	639	0	3225	21.5	2041	9.5	1965	3.2	1894	5	1832	7	1809	3.7	649	0.3	3202	20
Broan	403001	24	226	601	1	597	0.4	598	1.1	606	1.8	616	3.1	454	0.2	1484	50.8	585	0.7	587	0.3	596	0.7	600	1	596	1.3	455	0	1508	33.7
Broan	403001	30	87	1854	7.1	1642	5.5	1726	13.7	1834	11.2	1634	2.3	530	0.4	3192	24.1	1669	2.9	1807	13.3	1669	6.5	1692	12.6	1721	3.3	542	0.3	3226	20.4
Broan	403001	30	88	1824	8.1	1585	5.6	1644	4.2	1798	9.9	1656	6.2	542	1.1	3296	27.9	1601	0.8	1735	11.5	1674	9.8	1658	2.8	1625	3.6	544	0.5	3117	10.9
Broan	403001	30	88	1928	10.1	1705	4.5	1717	1.2	1940	14.6	1774	10.1	530	0.7	3312	22.7	1753	5.7	1862	15.3	1761	3.1	1757	5.4	1759	5.1	537	0.5	3181	16
Broan	403001	30	113	1269	3.5	1156	15.3	1161	1.5	1204	0.9	1252	4.1	525	0.6	2897	22.3	1151	7.4	1177	4	1174	0.4	1209	3.5	1210	1.7	531	0.8	2956	26.1
Broan	403001	30	115	1314	9.5	1243	3.4	1257	1	1288	7.5	1275	2.9	532	0.7	3016	20.8	1267	2.7	1270	1.4	1281	5.7	1268	3	1275	2.9	541	0.4	2888	24.7
Broan	403001	30	166	935	0.3	909	2.7	904	0.7	930	0.3	905	1.2	500	1.4	2173	25.6	921	2.4	929	0.8	911	1.5	951	2.2	929	1.1	503	0.4	2172	32.1
Broan	403001	30	167	942	1.1	914	0.9	918	0.5	944	1.7	931	1.8	505	0.6	2208	16.6	921	0.8	928	1.2	917	1.2	954	3.9	927	0.7	508	1	2205	17.1
Broan	403001	30	167	954	0.8	919	0.8	928	0.8	968	1.7	942	1.9	508	0.2	2226	25.3	920	0.4	922	0.6	919	0.8	988	0.4	934	0.3	514	0.8	2199	17.1

Table 4 shows the mean concentrations (and standard error of the mean) for each sampling port for a given range hood. Each row represents one five-minute steady state test period. There are two mounting heights and four nominal flow rates included for this range hood model. The chamber concentrations vary less for the higher capture efficiency tests than for the lower capture efficiency tests. But on the whole, the concentrations measured in the chamber indicate that the chamber is well-mixed.

The standard error of the mean for each test period indicates the temporal variability of the concentrations. The sampling location with the greatest temporal variability as a percentage of the concentration was in the exhaust stream. The mean and standard error of the mean of these concentrations are available for all tests in Appendices B and C.

VII. Summary

Although range hoods are required in codes and standards, their performance is highly variable. Currently, policy makers, builders, and homeowners alike lack a meaningful, robust metric with which to evaluate the efficacy of a given ventilation system. The tracer-gas-based steady-state capture efficiency test method developed in this study provides this needed metric for evaluating kitchen ventilation systems. The capture efficiency metric generated by this test represents the percentage of cooking pollutants that the range hood removes from the living space. The test results are repeatable (within +/- 0.5% CE) and have an uncertainty of less than 2% CE when using the recommended configuration.

Using the tracer gas approach demonstrated in this study requires a minimum of 4 chamber air changes to reach steady state conditions. Because of temporal variability in the tracer gas concentrations they should be averaged for at least 5 minutes after reaching steady state. Both of these recommendations will be incorporated into the ASTM test method.

In the course of developing this test method, eight under-cabinet range hoods were evaluated. The range hoods' capture efficiencies were measured at different airflow rates and mounting heights. In general, across all the tests, capture efficiency was positively correlated with airflow. However, the capture efficiencies across different configurations and models varied considerably for a given airflow. For instance, the measured capture efficiencies for the tests at approximately 150 cfm ranged from 65% to 90%. This variation suggests that range hood geometry and mounting height also have a significant impact on the efficacy of a kitchen ventilation system and moreover, that high capture efficiencies are possible to achieve at relatively low airflow rates with better hood design.

This study forms the basis for the development of an ASTM test method for evaluating kitchen ventilation systems. This method will be further refined and expanded upon to evaluate other kinds of kitchen ventilation, including island range hoods and downdraft systems. In time, the capture efficiency numbers measured using this method may be incorporated into residential ventilation standards such as ASHRAE 62.2 and will through code adoption lead to the dissemination of effective and well-utilized kitchen ventilation across the residential building stock.

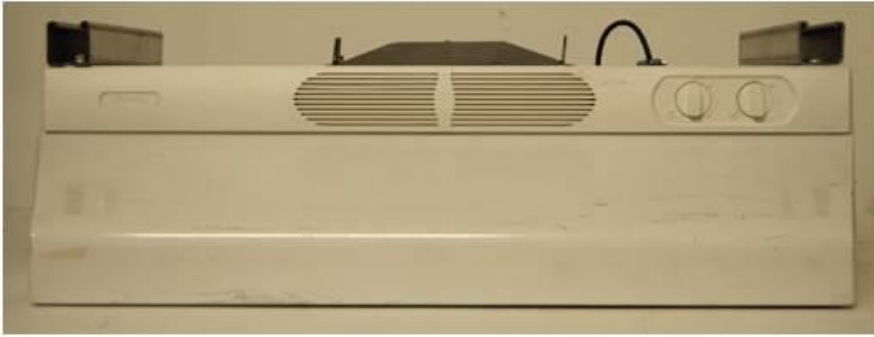
VIII. References

- ASHRAE Standard 62.2 *Ventilation and Acceptable Indoor Air Quality in Residential Buildings* (2013), ASHRAE, Atlanta, GA.
- ASTM (2005). ASTM F 1704-05 Standard Test Method for Capture and Containment Performance of Commercial Kitchen Exhaust Ventilation Systems. ASTM, West Conshohocken, PA.
- ASTM (2004). ASTM F 2029-04 Standard Test Method for Volumetric and Mass Flow Measurement in a duct using Tracer Gas Dilution. ASTM, West Conshohocken, PA.
- Awbi, H.B. (1991) *Ventilation of Buildings*, London, Chapman & Hall.
- Chen, C.J. and Rodi, W. (1980) *Vertical Turbulent Buoyant Jets - a Review of Experimental Data*, Oxford, Pergamon Press.
- Booth, B., & Betts, K. (2004). Cooking spews out ultrafine particles. *Environmental Science & Technology*, 38(8), 141a-142a.
- Delp, W. W., & Singer, B. C. (2012). Performance Assessment of U.S. Residential Cooking Exhaust Hoods. *Environmental Science and Technology*, 2012(46), 7.
- Dennekamp, M., Howarth, S., Dick, C. A. J., Cherrie, J. W., Donaldson, K., & Seaton, A. (2001). Ultrafine particles and nitrogen oxides generated by gas and electric cooking. *Occupational and Environmental Medicine*, 58(8), 511-516.
- Fugler, D. (1989). Canadian Research into the Installed Performance of Kitchen Exhaust Fans. ASHRAE Trans. Vol. 95, Pt. 1, pp. 753-758. ASHRAE, Atlanta, Ga.
- HVI (2015). Certified Home Ventilating Products Directory. Home Ventilating Institute publication 911. HVI, Morehead City, NC.
- IEC. (2005). International Standard IEC 61591. Household range hoods – methods for measuring performance. CEI/IEC 61591:1997+A1:2005. IEC, Geneva, Switzerland.
- Klug, V. L., Singer, B. C., Bedrosian, T., & D'Cruz, C. (2011). Characteristics of Range Hoods in California Homes – Data Collected from a Real Estate Web Site LBNL-5067E. Berkeley, CA: Lawrence Berkeley National Laboratory.
- Kosonen, R., Koskela, H, and Saarinen, P. (2006). Thermal Plumes of Kitchen Appliances: Idle Mode. *Energy and Buildings*, Vol. 38, pp. 1130-1139. Elsevier.
- Kuehn, T.H., Ramsey, J. Han, H., Perkivoich, M and Youssef, S. (1989). A Study of Kitchen Range Exhaust Systems. ASHRAE Trans. Vol. 95, Pt. 1, pp. 744-752. ASHRAE, Atlanta, Ga.
- Li, Y. and Delsante, A. (1996). Derivation of Capture Efficiency of Kitchen Range Hoods in a Confined Space. *Building and Environment*, Vol. 31., No. 5, pp. 461-468.
- Li, Y, Ho, E.C.W, Fracastoro, G.V. and Perino, M. (2001). A Short Note on Capture Efficiency of Kitchen Range Hoods in a Confined Space. *International Journal on Architectural Science*, Vol. 2, No. 2, pp. 46-52.
- Lunden, M.M, Delp, W.W. and Singer, B.C. 2014. Capture Efficiency of Cooking-Related Fine and Ultrafine Particles by Residential Exhaust Hoods. *Indoor Air*. DOI: 10.1111/ina.12118.

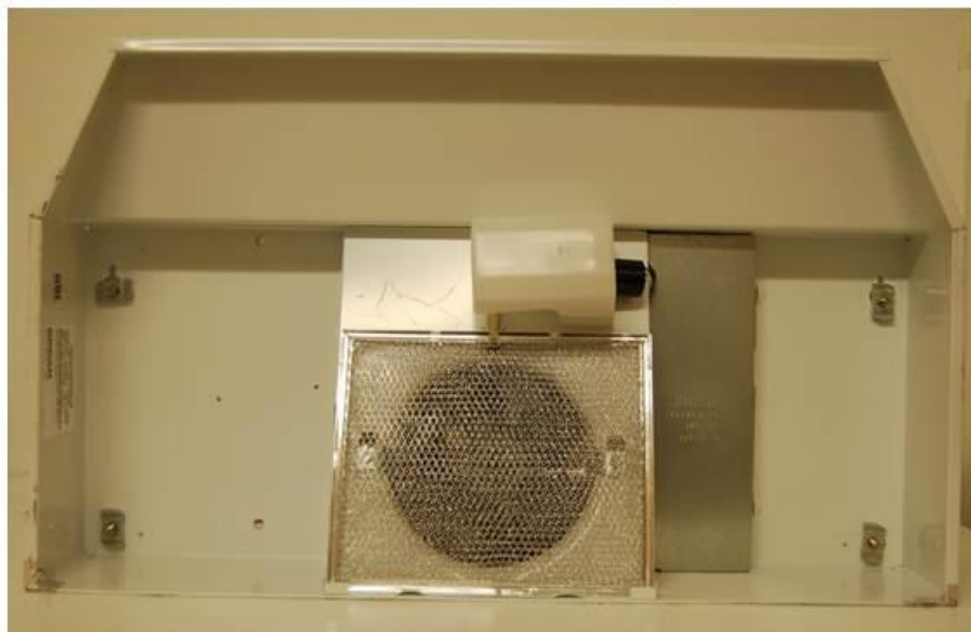
- Parrott, K., Emmel, J., & Beamish, J. (2003). Use of Kitchen Ventilation: Impact on Indoor Air Quality. *The Forum for Family and Consumer Issues*, 8(1).
- Rim, D., Wallace, L., Nabinger, S., & Persily, A. (2012). Reduction of exposure to ultrafine particles by kitchen exhaust hoods: The effects of exhaust flow rates, particle size, and burner position. *Science of the Total Environment*, 432, 350-356. doi: Doi 10.1016/J.Scitotenv.2012.06.015
- Simone, A., Sherman, M.H., Walker, I.S., Singer, B.C. Delp, W.W. and Stratton, J.C. 2015. Measurements of Capture Efficiency of Range Hoods in Homes. Proc. Healthy Buildings 2015.
- Singer, B. C., Apte, M. G., Black, D. R., Hotchi, T., Lucas, D., Lunden, M. M., & Sullivan, D. P. (2010). Natural Gas Variability in California: Environmental Impact and Device Performance - Experimental Evaluation of Pollutant Emissions from Residential Appliances. Berkeley, CA: Lawrence Berkeley National Laboratory.
- Singer, B. C., Delp, W. W., Price, P. N., & Apte, M. G. (2012). Performance of Installed Cooking Exhaust Devices. *Indoor Air: International Journal of Indoor Environment and Health*, 22(3), 11.
- Singer, B. C., Delp, W. W., & Apte, M. G. (2010). Experimental Evaluation of Installed Cooking Exhaust Fan Performance. *LBNL-4183E*.

Appendix A: Range Hood Models Tested

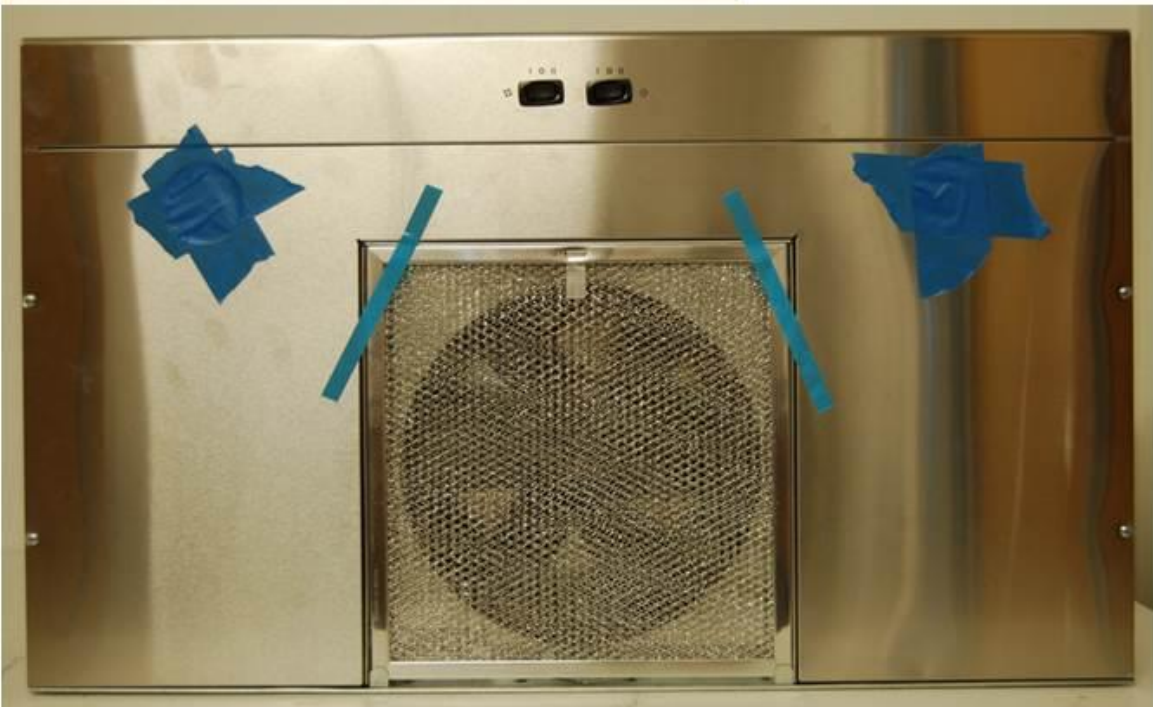
Make: Air King
Model: ESDQ1303
Mounting Height Range (in): 20-30
Depth (in): 19
Undercarriage Geometry: flat



Make: Broan
Model: 403001
Mounting Height Range (in): 24-30
Depth (in): 19
Undercarriage Geometry: deep sump



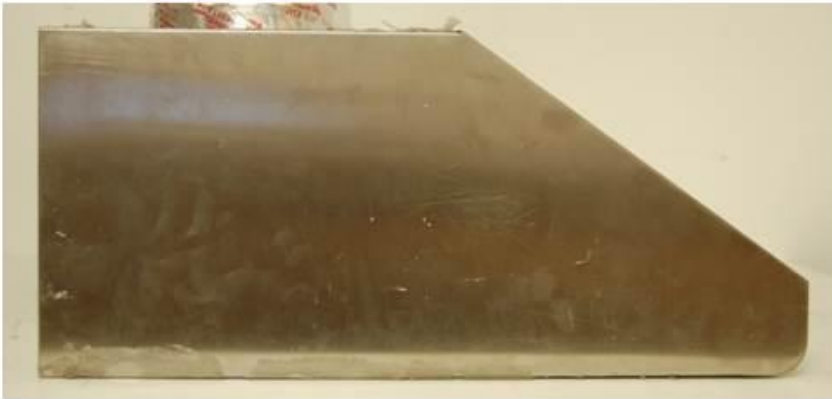
Make: Broan
Model: CBD130SS
Mounting Height Range (in): 18-24
Depth (in): 18
Undercarriage Geometry: flat



Make: Broan
Model: QP130WW
Mounting Height Range (in): 18-24
Depth (in): 18
Undercarriage Geometry: flat



Make: Cavaliere
Model: AP238PS633
Mounting Height Range (in): 27-30
Depth (in): 22
Undercarriage Geometry: shallow sump



Make: Panasonic
Model: NNSD277SR
Mounting Height Range (in): >12
Depth (in): 15
Undercarriage Geometry: flat



Make: Sakura
Model: U2F
Mounting Height Range (in): 24-32
Depth (in): 25
Undercarriage Geometry: shallow sump



Make: Vent-a-Hood
Model: B100
Mounting Height Range (in): 24-27
Depth (in): 21
Undercarriage Geometry: deep sump

